University of California, San Diego

Models of TDP-43 Proteinopathy in ALS / FTD and RNA targeting using CRISPR / Cas9

A dissertation submitted in partial satisfaction of the requirements for the degree Doctor of Philosophy

in

Biomedical Sciences

by

Elaine C. Pirie

Committee In Charge

Professor John Ravits, Chair
Professor Eugene Yeo, Co-Chair
Professor Xiang Dong Fu
Professor Christina Sigurdson
Professor Stephen Wagner

2017

The Dissertation of Elaine C. Pirie is approved, and it is acceptable in quality and form for publication on micro film and electronically:

_____

_____

_____

_____ Co- Chair

_____Chair

University of California, San Diego

2017

Dedication

This dissertation is dedicated to my husband, Andrew Anfora
and all our family

Epigraph

“Good decisions are just bad decisions you didn’t get to make”

e horne and j comeau, A Softer World

Table of Contents

List of Figures

Acknowledgements

First and foremost, I would like to thank my family for supporting and believing in me throughout this weird, winding graduate school path. I would especially like to thank my husband Andrew Anfora and my parents Phyllis Pirie, James Pirie and Linda Eells. Thanks for sticking with me everyone, I could not have done it without you.

Many, many thanks are owed to my co-advisors, John Ravits and Gene Yeo. I burst into their worlds unexpectedly and they have handled my sudden transition to their labs with grace and good humor.

Thank you so much to everyone in Stuart Lipton's lab, especially Tomohiro Nakamura, Olga Prihodko, Waseem Ahktar, and Chang-ki Oh.

Finally, I would also like to thank my friends in the Yeo lab. This literally would not have happened without your support, understanding, and astonishing amounts of candy. Special thanks to Julia Nussbacher, Ranjan Batra, and David Nelles, all of whom remained pretty certain I could do a PhD even when I didn't think so. Special shout out to Vu Nguyen, my all-star undergrad who probably never wants to hear the word "miniprep" ever again.

Chapter 3 is a modified adaptation of the material as it appears in: Elimination of Toxic Microsatellite Repeat Expansion RNA by RNA-Targeting Cas9. Ranjan Batra, David Nelles, Elaine Pirie, Steven Blue, Ryan Marina, Harrison Wang, Issac Alexander Chaim, James Thomas, Nigel Zhang, Vu Nguyen, Stefan Aigner, Sebastian Markmiller, Guangbin Xia, Kevin Corbett, Maurice Swanson, Gene Yeo. The dissertation author was the second author of this paper.

Vita

2008 Bachelor of Science, in Biology, University of Wisconsin, Madison

2017 Doctor of Philosophy, University of California, San Diego

Publications

Arnold, C. N., **Pirie, E**., Dosenovic, P., McInerney, G. M., Xia, Y., Wang, N., . . . Beutler, B. (2012). A forward genetic screen reveals roles for Nfkbid, Zeb1, and Ruvbl2 in humoral immunity. Proc Natl Acad Sci U S A, 109(31), 12286-12293. doi:10.1073/pnas.1209134109

Brandl, K., Tomisato, W., Li, X., Neppl, C., **Pirie, E**., Falk, W., . . . Beutler, B. (2012). Yip1 domain family, member 6 (Yipf6) mutation induces spontaneous intestinal inflammation in mice. Proc Natl Acad Sci U S A, 109(31), 12650-12655. doi:10.1073/pnas.1210366109

Nakamura, T., Prikhodko, O. A., **Pirie, E**., Nagar, S., Akhtar, M. W., Oh, C. K., . . . Lipton, S. A. (2015). Aberrant protein S-nitrosylation contributes to the pathophysiology of neurodegenerative diseases. Neurobiol Dis, 84, 99-108. doi:10.1016/j.nbd.2015.03.017

Park, H. J., Stokes, J. A., **Pirie, E**., Skahen, J., Shtaerman, Y., & Yaksh, T. L. (2013). Persistent hyperalgesia in the cisplatin-treated mouse as defined by threshold measures, the conditioned place preference paradigm, and changes in dorsal root ganglia activated transcription factor 3: the effects of gabapentin, ketorolac, and etanercept. Anesth Analg, 116(1), 224-231. doi:10.1213/ANE.0b013e31826e1007

Siggs, O. M., Arnold, C. N., Huber, C., **Pirie, E**., Xia, Y., Lin, P., . . . Beutler, B. (2011). The P4-type ATPase ATP11C is essential for B lymphopoiesis in adult bone marrow. Nat Immunol, 12(5), 434-440. doi:10.1038/ni.2012

Siggs, O. M., Berger, M., Krebs, P., Arnold, C. N., Eidenschenk, C., Huber, C., **Pirie, E**., Beutler, B. (2010). A mutation of Ikbkg causes immune deficiency without impairing degradation of IkappaB alpha. Proc Natl Acad Sci U S A, 107(7), 3046-3051. doi:10.1073/pnas.0915098107

ABSTRACT OF THE DISSERTATION

Models of TDP-43 Proteinopathy in ALS / FTD and RNA targeting using CRISPR / Cas9

By

Elaine C. Pirie

Doctor of Philosophy in Biomedical Science

University of California, San Diego

Professor John Ravits, Chair
Professor Gene Yeo, Co-Chair

Misregulation of RNA processing is a major component of the related neurodegenerative diseases Amyotrophic Lateral Sclerosis and Frontotemporal Degeneration. TDP-43 is an RNA binding protein and the primary pathological finding in both diseases. Post-translational modification of TDP-43 by direct S-nitrosylation of cysteines 173 and 175 leads to disulfide bond formation and loss of solubility in ALS / FTD models. Further, TDP-43 aggregation may be able to induce nitrosative stress within the cell, leading to further loss of solubility. We present models of TDP-43 aggregation that demonstrate TDP-43 is capable of propagating between cells quantifiably, spreading disease-associated aggregates. C9orf72 is the most common genetic cause of ALS / FTD, and here we establish a CRISPR / Cas9 technology capable of tracking and degrading RNA foci found in in myotonic dystrophy and C9 ALS. Our findings provide a novel framework for therapeutics targeted at TDP-43 aggregation and RNA toxicity.

Introduction

Frontotemporal lobar degeneration (FTD) and amyotrophic lateral sclerosis (ALS) are both age-related neurodegenerative diseases characterized by localized neurodegeneration, eventually resulting in death (Chen-Plotkin, Lee, & Trojanowski, 2010). The age-of-onset for both diseases is between 40 and 60 years of age. FTD is caused by deterioration of the frontal lobe often extending into the temporal lobe, leading to cognitive decline, aphasia and dementia (McKhann et al., 2001). It is thought to represent the second most common cause of dementia under the age of 65 due to genetic mutation (McKhann et al., 2001). ALS is a degenerative motor neuron disease in which both the upper and lower motor neurons deteriorate, leading to muscle atrophy, and is the most common form of neuromuscular disease in the world (E. B. Lee, Lee, & Trojanowski, 2011). Both diseases feature protein aggregates in the cytoplasm of affected cells (Neumann et al., 2006). Interestingly, about 50% of ALS patients eventually develop cognitive decline, and 15% of FTD patients develop motor neuron disease (Talbot & Ansorge, 2006). In 2006, it was discovered that a major component of these aggregates in nearly all cases of ALS and in the most common subtype of FTD was an RNA binding protein called trans-activation response DNA binding protein 43 kDa, or TDP-43 (Neumann et al., 2006).

TDP-43 was first discovered as a repressor of HIV-1 transcription. While TDP-43 is capable of binding DNA directly, it is now known to be a primarily

RNA-binding protein that regulates the repression, stabilization, and splicing of many mRNAs (Winton et al., 2008). Structurally, TDP-43 is made up of two RNA recognition motifs, RRM1 and RRM2, as well as a long glycine-rich tail (Fig. 1), with the majority of known TDP-43 mutations in the C-terminal tail (Geser, Martinez-Lage, Robinson, et al., 2009). There is no clear binding motif on the RNA targets of TDP-43, but it appears to preferentially bind UG repeats in introns (Tollervey et al., 2011).

As mentioned above, TDP-43 is also a major component of the inclusions that characterize ALS, FTD, and a group of more rare disorders known as the "TDP-43 proteinopathies." Its exact role in these conditions is not known, but mutations in the TDP-43 gene, TARDBP, have been found in both familial and sporadic forms of these diseases, suggesting a causative role for TDP-43 rather than a consequential one (Tollervey et al., 2011) (Dewey et al., 2012). There is now emerging evidence that in addition to being a prominent feature in ALS and some forms of FTD, TDP-43 pathology is a secondary feature in a wide variety of neurodegenerative disorders, including Alzheimer's disease (AD), Parkinson's disease (PD), and Huntington's disease (HD) (Geser, Martinez-Lage, Kwong, Lee, & Trojanowski, 2009). However the extent to which TDP-43 aggregation impacts symptoms in these diseases is not known, and mouse models have so far not been able to give good insight into the disease pathogenesis.

In human disease models, TDP-43 has been shown to be increasingly insoluble and mislocalized to the cytoplasm rather than the nucleus (Dewey et al., 2012). It may co-localize with cytoplasmic stress granules and is also more

highly phosphorylated and ubiquitinated. Evidence suggests that while phosphorylation occurs early in the disease process, ubiquitination does not occur until after aggregates form (Neumann et al., 2006) (Dewey et al., 2012). It is unclear whether TDP-43 aggregates have a gain-of-function toxicity or simply prevent TDP-43 from carrying out its normal role (Tollervey et al., 2011). The mechanism causing TDP-43 aggregation is not known, and more research into its causes and consequences may have a major impact on our understanding of neurodegenerative diseases.

Aggregation of TDP-43 in ALS / FTD raises intriguing possibilities in disease pathogenesis, considering TDP-43 itself exhibits substantial prion-like qualities: The C-terminal domain of TDP-43 has a proposed prion-like structure due to its asparagine and glutamine rich sequence (Fuentealba et al., 2010) and, intriguingly, essentially all ALS-causing genetic mutations in TARDBP are clustered in this 3´ region (Pesiridis, Lee, & Trojanowski, 2009). Recombinant TDP-43 has been shown to induce aggregation in cell culture via an apparent seeding mechanism (Furukawa, Kaneko, Watanabe, Yamanaka, & Nukina, 2011), as has insoluble TDP-43 from FTD and ALS patient CNS ((Nonaka et al., 2013). These reactions also resulted in toxicity and cell death in the target cells. Although several models of TDP-43 mediated toxicity have been proposed (Janssens & Van Broeckhoven, 2013; Nonaka, Kametani, Arai, Akiyama, & Hasegawa, 2009) (Brettschneider et al., 2014), the mechanisms of TDP-43 propagation and aggregation are still unclear and very little attention has been directed to elucidating the biology of its propagation. In particular, the

mechanisms of TDP-43 release and uptake remain unclear. It is important to develop models for TDP-43 aggregation and prion-like propagation through the nervous system to better understand the mechanisms of ALS pathogenesis and tailor future therapeutic approaches.

That TDP-43 is an RNA binding protein cannot go unremarked, as evidence increasingly implicates RNA misregulation in ALS / FTD. 1. The primary / only pathological hallmark of ALS is TDP-43 aggregation, with mutations in TDP-43 being causative (Sreedharan et al., 2008) (Daoud et al., 2009). 2. RNA binding proteins generally are associated in ALS pathogenesis, as many ALS-causing mutations occur in RBPs, leading to RNA misregulation (Nussbacher, Batra, Lagier-Tourenne, & Yeo, 2015) (Mohagheghi et al., 2016). 3. The most common genetic cause of ALS / FTD is the C9orf72 hexanucleotide repeat expansion, which triggers the production of RNA foci in the nucleus in the cells of patients with the disease (DeJesus-Hernandez et al., 2011). The exact mechanism by which this expansion induces ALS / FTD is not clear, but RNA foci and other downstream effects of this RNA appear to play a major role in disease pathogenesis (Belzil, Gendron, & Petrucelli, 2013). Appropriate regulation of RNA, based either on correction of RBP pathology or other technologies, may provide a major therapeutic benefit to patients with ALS / FTD.

RNA misregulation is at the root of other neurological / neuromuscular diseases. The microsatellite repeat – expansion diseases are disorders produced by an expansion of short repetitive nucleotide base sequences within the genome, and result in accumulations of pathogenic RNA foci in affected cells

(Cleary & Ranum, 2014) (Usdin, 2008). These diseases include the C9orf72 repeat expansion discussed above, as well as myotonic dystrophy (Sicot & Gomes-Pereira, 2013). Myotonic Dystrophy (DM) is a disease affecting multiple organ systems in which pathology develops in skeletal and cardiac muscle in addition to the CNS. The genome of DM patients contain an expansion of the sequence CTG (DM1) or CCTG (DM2), and this expanded nuclear transcript is maintained as RNA foci in the nucleus (Goodwin et al., 2015). These foci sequester an assortment of proteins capable of binding RNA, including HNRP, STAU1, CUGBP1 and ETR3-like (CELF), and muscleblind- like (MBNL) (K. Y. Lee et al., 2013). The sequestration of MBNL and other RNA binding proteins leads to misregulation of alternative splicing (AS) in an array of RNA transcripts, which contributes to the multi-systemic nature of this disease (Goodwin et al., 2015).

The C9orf72 hexanucleotide repeat is the most common genetic causes of both familial and sporadic ALS (Talbot & Ansorge, 2006). There are three main hypotheses regarding the mechanism of cell stress / death in the C9 repeat expansion: 1. Loss of function of the C9orf72 protein. The function of C9orf72 is not clear, but the protein has some homology with proteins involved in shuttling (Mackenzie, Frick, & Neumann, 2014). There are multiple isoforms, as the protein can be alternatively spliced (Almeida et al., 2013). However, C9orf72 knockout mice do not recapitulate the effects of disease (Koppers et al., 2015). This makes loss of C9orf72 function an unlikely primary cause of the symptoms of ALS / FTD. 2. Toxic RNA foci: The accumulated RNA foci may have a toxic

gain of function which induces cell stress, or may be sequestering required RNA binding proteins in the nucleus, as in DM1 (Haeusler, Donnelly, & Rothstein, 2016). 3. Toxic dipeptide repeats: the expansion transcript is translated in both the sense (GGGGCC) and antisense (CCCCGG) direction via repeat-associated, non-ATG dependent (RAN) translation, five dipeptide repeats – three in each direction (GP is present in both directions) (Mackenzie et al., 2013) (Cleary & Ranum, 2014).

Both DM and C9 ALS/FTD are neurodegenerative diseases featuring RNA foci accumulation in the nucleus (Belzil et al., 2013). While much about the etiology of these diseases remains unclear, targeting of the RNA foci is an intriguing research area.

Here, we present multiple models and techniques focused on the regulation of RNA in ALS / FTD via RBPs and novel biotechnology. We show that TDP-43 solubility is directly regulated by nitrosative stress, leading to aggregation in cell models of ALS / FTD in a manner similar to that seen in FTD patient brain. Further, we show that TDP-43 may be able to induce further nitrosative stress within the cell, possibly inducing increasing aggregation. We also establish a preliminary model for quantifying TDP-43 propagation in a cell culture system, which may be used for downstream screens in order to better understand TDP-43 spread. Finally, we characterize a novel biotechnology and demonstrate its ability to track and degrade RNA foci in vivo, further establishing its therapeutic potential in patients with microsatellite repeat diseases.

Chapter 1: S-Nitrosylation of TDP-43

1.1 Rationale

Recent evidence from the laboratory of Virginia Lee and John Trojanowski suggests that oxidative stress (due to reactive oxygen species (ROS)) can cause TDP-43 aggregation and decrease its activity in vitro (Cohen, Hwang, Unger, Trojanowski, & Lee, 2012). This indicates that TDP-43 is a stress-responsive factor and that therapeutic strategies for affected patients could possibly utilize antioxidant-based treatments.

As first discovered by Dr. Lipton's group and colleagues, S-nitrosylation represents the reaction of a nitric oxide (NO) moiety with a protein thiol group that regulates protein function (Akhtar, Sunico, Nakamura, & Lipton, 2012). Under normal conditions ROS and reactive nitrogen species (RNS) are present at low levels in the cell, functioning as signaling mechanisms in several neuroprotective pathways (Nakamura & Lipton, 2013). In pathological conditions production of ROS and RNS is increased, leading to oxidative and nitrosative stress. NO-related species represent RNS that are known to covalently react with a cysteine thiol group (or more properly thiolate anion) in a protein, causing a post- translational modification and thus affecting protein activity (Akhtar et al., 2012). Such proteins are known as "SNO-proteins" (representing Cys-S-NO).

Both exogenous and endogenous mechanisms can cause pathological nitric oxide concentrations in the brain. Exogenous mechanisms include environmental exposure to NO (e.g., nitrates or other RNS in air pollution and high-density automobile traffic), and also to pesticides such as rotenone and

paraquat/maneb (Betarbet et al., 2000). Interestingly, epidemiological studies of ALS patients have suggested a link between exposure to certain pesticides and the development of ALS (Kamel et al., 2012).

One of the principal ways endogenous NO causes S-nitrosylation is via activation of NMDA-type glutamate receptors (NMDARs). Many excitatory synapses in the brain contain NMDAR-operated channels activated by glutamate (and co-agonist glycine or D-serine). Activation of these channels leads to calcium influx into the neuron, which triggers activation of nNOS (neuronal nitric oxide synthase) to convert L-arginine to citrulline, thereby producing NO (Sattler et al., 1999). Pathological hyperactivation of NMDARs leads to the overproduction of NO, resulting in aberrant S-nitrosylation reactions on proteins that would not normally become S-nitrosylated and can thus compromise a number of proteins critical to cell function (Nakamura & Lipton, 2013).Once nitrosylated, NO often represents a good “leaving” group in chemical parlance, as NO will react with other electron donors if the Gibbs free energy is thereby reduced. When this occurs, the NO group is often replaced by ROS reacting with the same thiol group, which, presumably because of a conformational change in the protein, is now more reactive (Sattler et al., 1999) (Lopez-Sanchez, Lopez-Pedrera, & Rodriguez-Ariza, 2014).

Alternatively, if vicinal thiols are present, when NO leaves a thiol, a disulfide bond may form (Hess, Matsumoto, Kim, Marshall, & Stamler, 2005).

Proteins with S-nitrosylated cysteines may then aggregate, for example, if intermolecular disulfide bonds connect them.

Not all cysteines are capable of being S-nitrosylated. Cysteines that are surrounded by a so-called amino acid “SNO-motif” are more likely candidates. The SNO-motif is comprised of flanking acidic and basic amino acids, which affect the deprotonation of the thiol to the thiolate anion, which is capable of binding NO (Andre, dos Santos, & Rando, 2016; Hess et al., 2005).

Recently, oxidative stress was shown to cause TDP-43 aggregation in vitro (Cohen et al., 2012). Along these lines, Cohen et al. determined that exposure of COS7 cells to hydrogen peroxide and arsenite led to insoluble TDP-43 formation. They went on to determine using 14-iodoacetate that cysteine residues were the target of oxidative stress in TDP-43. They were unable to determine which cysteine(s) were involved, nor through what mechanism of aggregation occurred. Interestingly, another group determined that the use of methylene blue could prevent TDP-43 aggregation in vitro (Yamashita et al., 2009). Methylene blue is known to inhibit nitric oxide synthase, among other actions. Taken together, these data support the notion that TDP-43 aggregates in response to oxidative stress, and that NO might play a role in such aggregation.

Results

1.2 TDP-43 is capable of being S-Nitrosylated

We first exposed 14 day old rat primary cortical neurons to 200uM s-nitrosocysteine, an exogenous NO donor produced by the reaction of cysteine

and sodium nitrite. After one hour the cells were assessed by a biotin-switch assay: free thiols were blocked with MMTS, any nitric oxide was reduced away using ascorbate, and the free thiols were biotinylated. Streptavidin pulldown and subsequent western blot showed an increased amount presence of biotinylated TDP-43 over control samples (Figure 1A), indicating this protein was being S-nitrosylated. We next tested an endogenous model of S-nitrosylation using HEK cells modified to express neuronal nitric oxide synthase. As calcium influx activates nNOS, the cells were exposed to A23187, a calcium ionopore, overnight at 37C. Subsequent biotin switch once again demonstrated increased biotinylation of TDP-43 after treatment, indicating that it was S-nitrosylated (Figure 1B). To further confirm the ability of TDP-43 to be S-nitrosylated by endogenous NOS, we utilized the existing NMDA receptors on the rat primary cortical neurons. We exposed 21 day old rat primary cortical neurons to 50uM NMDA for 20 minutes and then allowed the cells to rest for three hours. Biotin-switch again showed an increase in SNO-TDP-43 formation (Figure 1C). Recombinant TDP-43, amino acids 1-265, was generated and exposed to s-nitrosocysteine. SNO-TDP-43 was again detected by biotin switch (Figure 1D). The recombinant protein was then exposed to s-nitrosocysteine and submitted for top-down mass spectrometry, which does not require protein cleavage and allows detection of post translational modifications. Mass spec detected a 29KD shift in the treated recombinant TDP-43 sample, which is the expected size of an addition of nitric oxide (Figure 1E).

1.3 S-Nitrosylation of TDP-43 induces in Aggregation

Previous work has indicated that in the CNS of patients affected by ALS / FTD, TDP-43 protein is concentration is increased in the insoluble fraction in cell lysate (Ayala et al., 2008; Furukawa et al., 2011). To see if S-nitrosylation induced TDP-43 aggregation, we treated 14 day old rat primary cortical neurons with 200uM SNOC and fractionated the resulting cell lysate as in (Cohen et al., 2012). Using western blot, we detected a substantial increase in TDP-43 in the insoluble fraction, while the soluble fraction remained unchanged (Figure 2A). We then exposed 21 day old rat primary cortical neurons to NMDA and fractionated the lysate. Interestingly, there was an increase in the insoluble TDP-43 fraction as expected, but this increase was attenuated in another sample where L-NAME, an inhibitor of nNOS, had been added (Figure 2B). This indicated that the insolubility of TDP-43 in these cells was the direct result of NOS-mediated nitric oxide generation.

We next treated SH-SY5Y cells, an immortalized glioblastoma cell line (Xie, Hu, & Li, 2010), with SNOC and fixed them for immunofluorescence. An antibody against TDP-43 detected the presence of TDP-43 outside the nucleus in the treated cells. Intriguingly, TDP-43 co-localized with TIAR, an RNA binding protein and stress granule marker (Figure 2C). Stress granules are aggregates of RNA and protein that accumulate in the cytoplasm during cell stress and have been implicated in the development of ALS / FTD (Dewey et al., 2012).

In order to establish if ALS / FTD associated mutations might make patients more vulnerable to nitrosative stress, we treated hiPSC derived motor

neurons from a control patient and three patients with ALS / FTD causing mutations. As expected, SNOC treatment on these motor neurons induced an increase in the insoluble TDP-43 detected in control condition and two of the ALS / FTD mutant lines. Unexpectedly, one line had an extreme reaction to SNOC treatment, producing a surprisingly large amount of insoluble TDP-43, including high molecular weight TDP-43 and cleaved fragments, both of which are seen in patient fractions (Figure 2D). This indicated that genotype may be an important determinant of a patients ability to cope with environmental nitrosative insult.

1.4 Cysteines 173 and 175 are the S-nitrosylated Cysteines on TDP-43

While TDP-43 contains six cysteines, previous work has shown that only four are likely to be involved in cysteine oxidation (Cohen et al., 2012). To investigate if these four cysteines (173, 175, 198, 244) were involved in TDP-43 S-nitrosylation, we generated plasmids with point mutations switching these four cysteines with alanine, which is structurally identical to cysteine but is missing the thiol group and is therefore not capable of being S-nitrosylated. We next transfected these plasmids, along with a wild-type TDP-43 control, into SH-SY5Y cells. Biotin-switch showed that when cysteines 173 and 175 were mutated to alanines SNO-TDP-43 was not formed. This indicated that TDP-43 is S-nitrosylated at these cysteines (Figure 3A).

1.5 Non-Nitrosylatable TDP-43 is less prone to aggregation, retains function and prevents cell death.

SH-SY5Y cells were transfected with wild – type and non-nitrosylatable TDP-43, exposed to SNOC and the lysate was fractionated. Western blot showed that there was less insoluble TDP-43 in cells transfected with the mutant (Figure 3B). HDAC6 mRNA is known to be stabilized by TDP-43, and so can be used as a measure for TDP-43 activity. Cells were transfected with wild-type TDP-43, non-nitrosylatable mutant TDP-43, SiTDP-43, and SiControl, then exposed to SNOC. QPCR was used to assess the amount of HDAC6 mRNA (Fiesel et al., 2010). As expected, knockdown of TDP-43 using SI resulted in HDAC6 reduction (Figure 3C). However cells transfected with non-nitrosylatable mutant TDP-43 expressed significantly more HDAC6 mRNA after SNOC treatment than those with wild-type TDP-43. This indicated that TPD-43 functionality was retained during nitrosative stress.

In order to assess whether non-nitrosylatable TDP-43 would protect cells from nitric oxide induced cell death, we transfected SH-SY5Y cells with both wild-type and non-nitrosylatable mutant TDP-43 and exposed to SNOC at increasing concentrations overnight. We then assessed cell death using a TUNEL assay, where the ends of nicked DNA is labeled with a fluorescent dye. At low levels of nitric oxide there was no difference in the amount of cell death observed between the wild-type and mutant conditions. However at 100uM SNOC, significantly more cell death was observed in the cells transfected with wild-type TDP-43 (Figure 3D). This indicated that non-nitrosylatable TDP-43 was protective against cell death induced by nitric oxide.

1.6 S-nitrosylation of TDP-43 Induces Reducing-Agent Sensitive High Molecular Weight TDP-43

Rat primary cortical neurons were exposed to SNOC and fractionated, then the lysate was run on a Western blot in reducing and non-reducing conditions. In the non-reducing conditions, high molecular weight TDP-43 was observed. Intriguingly this was not observed in reducing conditions (Figure 4A). Similar high molecular weight TDP-43 was also observed in non-reducing conditions in the recombinant protein (Figure 4B), indicating the HMW form of TDP-43 was a direct result of being S-nitrosylated.

To directly test if the HMW TDP-43 is a product of SNO-TDP-43, we treated rat primary cortical neurons with SNOC and isolated the lysate at 10 and 40 minutes. By biotin-switch, 10 minutes after treatment a substantial amount of SNO-TDP-43 was observed, as was a small amount of HMW TDP-43. After 40 minutes the amount of HMW TDP-43 was significantly increased while the amount of SNO-TDP-43 was reduced (Figure 4C). This indicated that SNO-TDP-43 is the initial product of S-nitrosylation and further downstream affects result in HMW TDP-43.

Nitric oxide is a well-known leaving group, and S-nitrosylation is known to be a transient reaction (Hess et al., 2005). The free thiolate anion generated by the cysteine once the nitric oxide moiety departs is capable of further oxidation reactions, including disulfide bond formation. Disulfide bonds are easily broken by most reducing agents (Begg & Speicher, 1999). For this reason we suspected

the high molecular weight TDP-43 was the result of disulfide bond formation, leading to aggregation.

1.6 Reducing Agent Sensitive TDP-43 is Detected in FTD Patient Brain

Cortex from three FTD patients and three controls was obtained and lysate was processed for western blot. In non-reducing conditions, high molecular weight smears are observed after probing for TDP-43. These smears dissipate when the same lysate is run in reducing conditions (Figure 4D).

1.7 TDP-43 May Induce Nitrosative Stress

Aggregated protein is known to be a source of nitrosative stress in the cell via ER stress and the UPR pathways (Nakato et al., 2015). In order to test if aggregated TDP-43 was capable of inducing nitrosative stress, we transfected TDP-43 plasmid in SH-SY5Y cells in order to overexpress it and induce aggregation. Two days after transfection we tested the cell media for byproducts of nitric oxide using the Griess reaction, a well-known assay used for detecting NO2. The Griess reaction showed increased fluorescence in cells transfected with TDP-43 (Figure5A). This fluorescence was attenuated in cells that had been treated with the NOS inhibitor L-NAME. This indicated that TDP-43 overexpression was able to induce the formation of nitric oxide, probably via endogenous NOS.

We further tested the ability of TDP-43 to induce nitric oxide production using recombinant (1-265) TDP-43 protein. Recombinant protein was added to

the media of rat primary cortical neurons and incubated overnight. The cells were then subjected to DAF-FM, a fluorescent method for detecting nitric oxide production within a cell. Interestingly, cells exposed to recombinant TDP-43 showed increased fluorescence during DAF-FM as opposed to cells exposed to a control protein (Figure 5B).

1.8 Discussion

TDP-43 solubility and aggregation has been strongly implicated in the pathogenesis of ALS / FTD, however the signaling mechanisms responsible for these pathways are not well understood. Here we provide evidence that nitrosative stress potentially plays a crucial role in the loss of TDP-43 solubility. We demonstrate that TDP-43 is directly regulated by nitric oxide - induced disulfide bond formation which reduces its functionality. Further, we have presented evidence that TDP-43 is potentially involved in a feedback loop whereby aggregates are able to induce nitric oxide formation within the cell, leading to further loss of TDP-43 solubility (Figure 6). Thus, our data suggests that S-nitrosylation of TDP-43 represents a mechanism which directly contributes to the development of ALS / FTD.

Because nitric oxide represents a good leaving group, it is well known to be an upstream event which is capable of inducing further oxidative modifications, including disulfide bond formation. Intriguingly, nitrosative stress both in vivo and in vitro resulted in reducing agent - sensitive high molecular weight TDP-43, suggesting the presence of disulfide bonds. FTD patient cortex

revealed similar disulfide bond crosslinked high molecular weight TDP-43. It is not clear from our data whether these disulfide bonds are formed inter- or intra-molecularly, however either bond could alter the TDP-43s structural conformation resulting in increased aggregation propensity or increased kinase accessibility (Chiang et al., 2016). Supporting this hypothesis is our data establishing translocation of TDP-43 from the nucleus to the cytoplasm following nitrosative stress, as cytoplasmic TDP-43 is widely regarded as a molecular hallmark of ALS / FTD.

We report that TDP-43 solubility is readily regulated by disulfide bond formation at cysteines 173 and 175. This is consistent with previous reports describing TDP-43 disulfide bond formation in ALS mouse model and patient nervous system. Interestingly, (Lukavsky et al., 2013; Shodai et al., 2013) uncovered significant NMR shifts in this region of recombinant TDP-43 protein during stress, suggesting that the RRM1 induced aggregation may function as an upstream aggregation event. Our findings that non-nitrosylatable TDP-43 was less prone to nitric oxide - induced insolubility is bolsters this hypothesis.

Our data provides compelling evidence as to how S-nitrosylation may contribute to the pathogenesis of TDP-43 proteinopathy as seen in ALS / FTD. Previous work has identified NMDA activation by Abeta oligomers (Gu, Nakamura, & Lipton, 2010), leading to calcium influx which is able to activate nNOS and contribute to Alzheimer's Disease pathogenesis. Intriguingly, (Fang et al., 2014) demonstrated that oligomers of TDP-43 identified in FTD patient brain could be detected using antibody against Abeta oligomers, suggesting similar

structural morphology. We hypothesized that insoluble TDP-43 may be able to induce similar nNOS activation. Indeed, our data robustly demonstrated that overexpression of wild-type TDP-43 in SH-SY5Y cells increase nitric oxide metabolites detected in the media using the Greiss reaction. This increase was abrogated by treating the cells with L-NAME, which inhibits NOS activity. We further examined this hypothesis by measuring internal nitric oxide production in rat primary cortical neurons treated with recombinant TDP-43. Surprisingly the recombinant protein was not detected inside the target cells, however these cells displayed a significant increase in nitric oxide production. This suggests that TDP-43 may be able to interact with NMDA receptors in a manner similar to Abeta, thereby inducing nitric oxide production. This suggests a compelling mechanism whereby insoluble TDP-43, formed either by environmental stressors or genetic vulnerability, is able to induce the production of aberrant nitric oxide within the cell leading TDP-43 S-nitrosylation, disulfide bond formation, and further aggregation.

Overall this data suggests a novel regulatory mechanism impacting TDP-43 solubility and pathogenesis of ALS / FTD. Targeting this feedback loop may prove useful in therapeutics aimed at treatment of ALS / FTD.

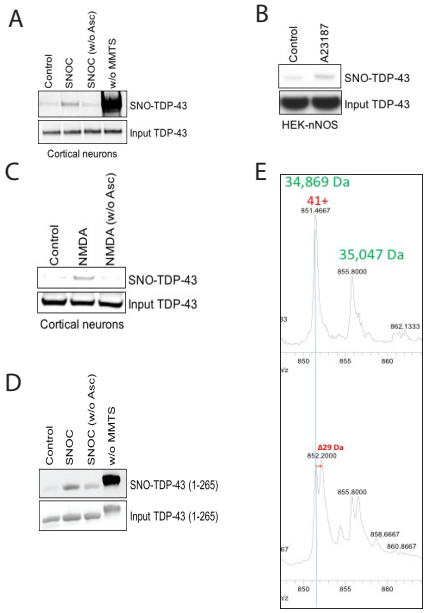

Figure 1: TDP-43 is Capable of being S-Nitrosylated

(A) Biotin-switch assay on 14 day old rat primary cortical neurons treated with 200uM SNOC for 1 hour. W/o asorbate is negative control, without MMTS represents a positive control. Antibody against TDP-43

(B) Biotin-switch assay on HEK cells expressing nNOS, treated O/N with calcium ionopore A27187. Antibody against TDP-43

(C) Biotin-switch assay on 21 day old rat primary cortical neurons treated with 50uM NMDA for 15 minutes, followed by 3 hours rest. Antibody against TDP-43

(D) Biotin-switch assay carried out on recombinant TDP-43 protein, amino acids 1-265, treated with 200uM SNOC for 20 min. Silver stain

(E) Top-down mass spec carried out on recombinant TDP-43 (1-265). Peaks represent the presence of protein of a particular size. Recombinant protein is present with and without initiating methionine. Top is control treated, bottom was treated with 200uM SNOC for 10 minutes.

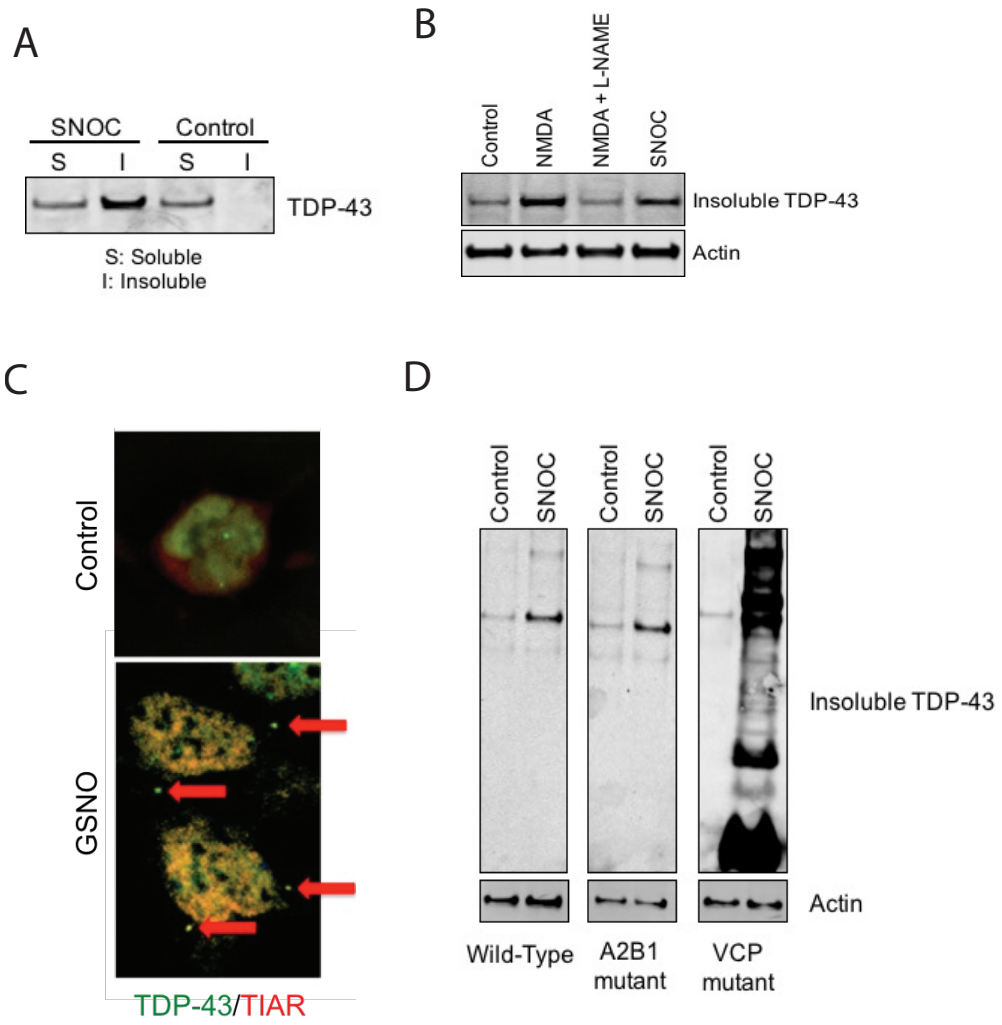

Figure 2: Nitrosative Stress Increases TDP-43 Insolubility
(A) SHSY5Y cells treated with 200uM SNOC for one hour were lysed in RIPA buffer and fractionated into soluble (S) and insoluble (I) fractions. Antibody against TDP-43.

(B) 21 day old rat primary cortical neurons were treated with 50uM NMDA for 15 minutes, then rested for 3 hours before harvest and fractionated. L-NAME is an inhibitor of nNOS

(C) SHSY5Y cells were treated with 200uM GSNO for 1 hour, then fixed and probed with antibody against TDP-43 (green) and stress granule marker TIAR (red). Arrows indicate cytoplasmic TDP-43.

(D) hiPSC derived motor neuron lines were treated with 200uM SNOC, then fractionated. Insoluble TDP-43 was probed by western blot.

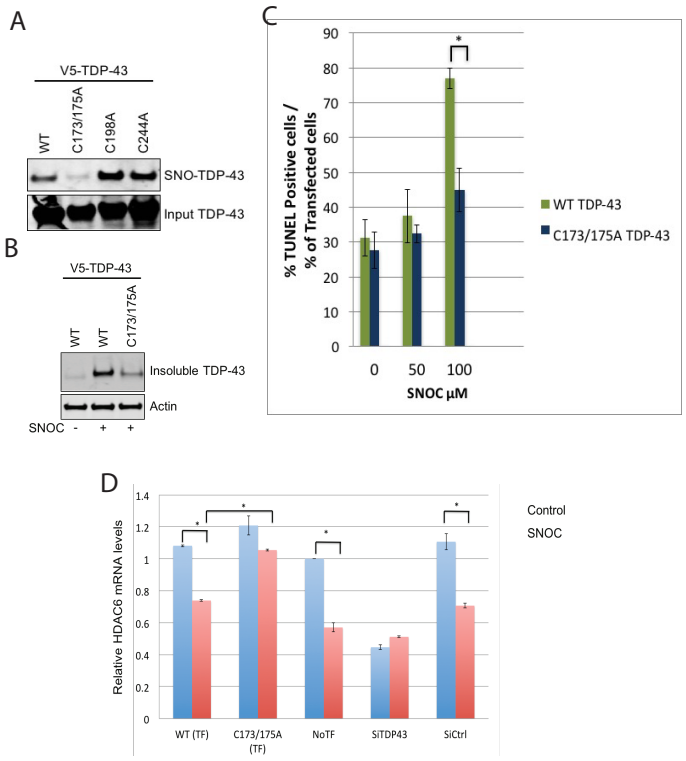

Figure 3: Cysteines 173 and 175 are S-Nitrosylated

(A) Point mutants of TDP-43 with a V5 tag were generated mutating Cysteine to Alanine. SHSY5Y cells were transfected with mutant and wild-type constructs, and after 24 hours the cells were exposed to 200uM SNOC for 1 hour. Cells were then lysed and biotin switch was carried out. Analysis done via western blot, using V5 antibody.

(B) Wild type TDP-43 and non-nitrosylatable TDP-43 mutant C173/5A were transfected into SHSY5Y cells, then exposed to 200uM SNOC for 1 hour where indicated. Cell lysate was fractionated and probed by western blot with V5 antibody.

(C) Wild type TDP-43 and non-nitrosylatable TDP-43 mutant C173/5A were transfected into SHSY5Y cells, which were then exposed to increasing concentrations of SNOC for 24 hours. Percent cell death was assessed by TUNEL. Students T test, p=0.0024

(D) Wild type TDP-43, non-nitrosylatable TDP-43 mutant C173/5A, siTDP-43 and siControl were transfected into SHSY5Y cells. 24 hours after transfection cells were exposed to 200uM SNOC for 1 hour, then rested for 12 hours. RNA was extracted and subjected to QPCR using probe against HDAC6 mRNA. 18S was used as housekeeping gene. Anova, p=0.00076

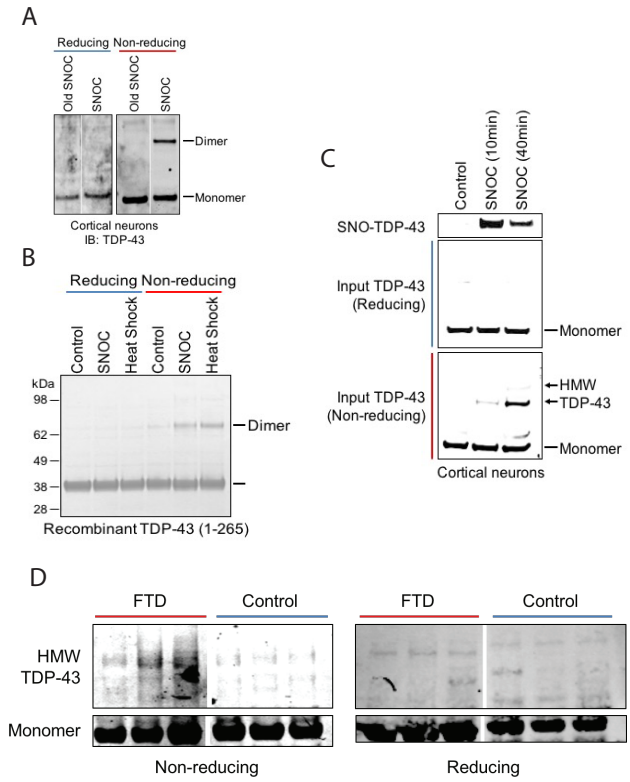

Figure 4: Nitrosative Stress Induces High Molecular Weight TDP-43

(A) 14 day old rat primary cortical neurons were treated with 200uM SNOC for 1 hour, then fractionated. The insoluble fraction was then probed for TDP-43 by western blot, using either 10% b-mercaptoethanol loading dye(reducing condition) or only loading dye (non-reducing condition).

(B) Recombinant 1-265 amino acid TDP-43 was treated with 200uM SNOC for 20 minutes, then loaded onto an SDS page gel in either 10% b-mercaptoethanol loading dye(reducing condition) or only loading dye (non-reducing condition). Analyzed by silver stain.

(C) Rat primary cortical neurons were treated with 200uM SNOC for either 10 or 40 minutes. SNO-TDP-43 formation was assessed by biotin-switch, while the input control sample was run using either 10% b-mercaptoethanol loading dye(reducing condition) or only loading dye (non-reducing condition).

(D) Frozen frontal cortex from FTD and control patients was lysed in RIPA buffer and probed for TDP-43 by western blot using either 10% b-mercaptoethanol loading dye(reducing condition) or only loading dye (non-reducing condition).

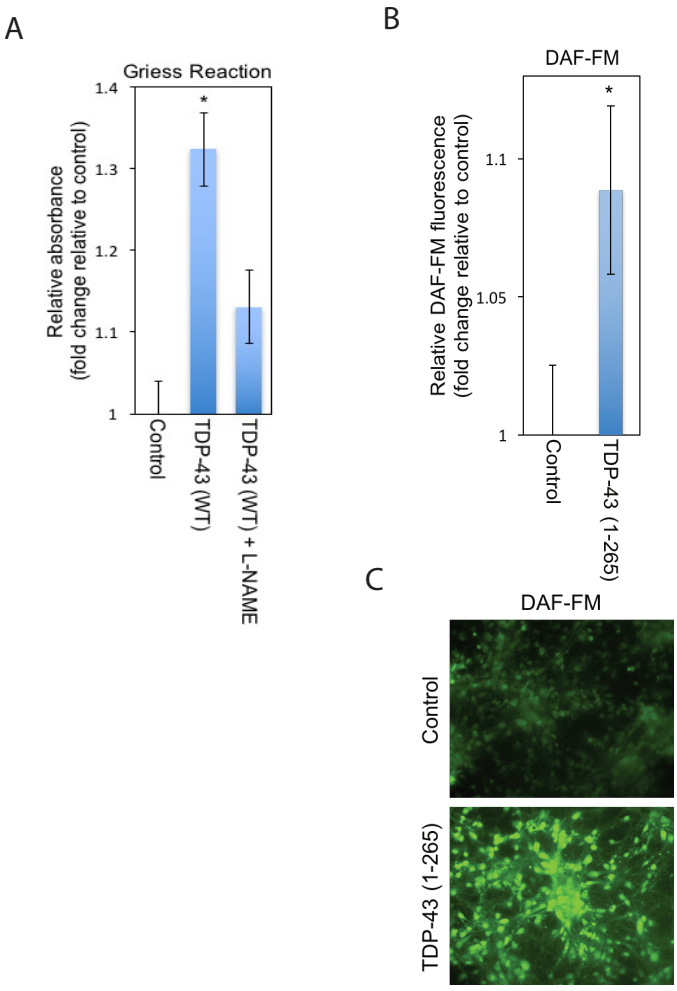

Figure 5: TDP-43 Induces Nitrosative Stress

(A) SH-SY5Y cells were transfected with wild-type TDP-43, then treated with L-NAME where indicated. After 72 hours the media was aspirated and subjected to the griess reaction. Fluorescence was measured on a plate reader at 625nm.

(B) Rat primary cortical neurons were treated with either 10ug recombinant 1-265 TDP-43 or control protein. After 24 hours cells were subjected to DAF-FM and fluorescence was measured.

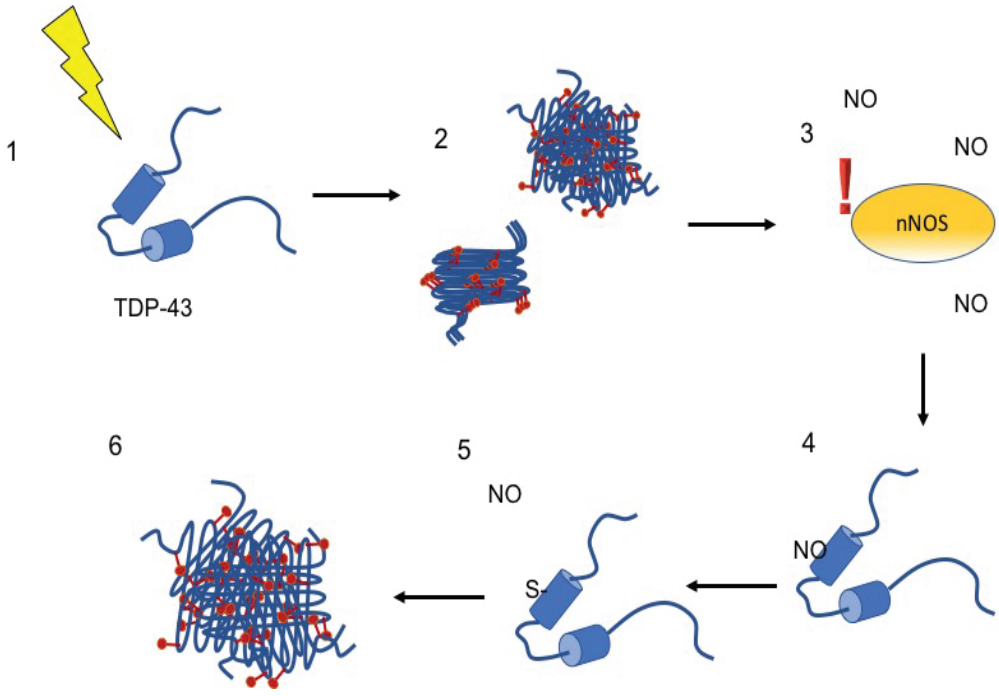

Figure 6: Potential Mechanism of SNO-TDP-43 Feedback Loop
(A) 1. An endogenous or exogenous stressor induces aggregation of TDP-43, which forms 2. aggregates or TDP-43 oligomers. These are able to 3. activate nNOS via the UPR, which produces nitric oxide. 54 The increase in cellular nitric oxide allows aberrant S-nitryoslation of TDP-43. 5. Nitric oxide leaves TDP-43, forming a reactive thiolate anion. 8. Downstream disulfide bond formation results in further aggregation of TDP-43

Materials and Methods

1.9 Plasmids and cell culture

Human TDP-43 was cloned into pCDNA3.1/V5 vector, and site-directed mutagenesis (QuickChange Lightning – Agilent) was used to create all cysteine to alanine mutations at residues 173, 175, 198 and 244 in the combinations indicated. Plasmids were transfected into SH-SY5Y cells using LTX (Invitrogen) as per the manufacturer's protocols. SH-SY5Y and HEK stably expressing nNOS cells were grown in Dulbecco's modified Eagle's medium supplemented with 10% fetal bovine serum and 1% L-glutamate. TDP-43 siRNA sequence was as follows: AACACTACAATTGATATCAAA and was transfected using RNAi Max reagent (Invitrogen) per the manufacturer's protocols. Primary neuronal cultures were prepared from E16-18 Sprague-Dawley rats and maintained in culture. Dissected cerebrocortices were treated with trypsin, and dissociated cells were plated on poly-L-lysine coated plates in D10C medium containing 25 mM glucose. Experiments were performed 14–21 days after plating.

1.10 Immunofluorescence

Cultured cells were plated using 100ng/uL fibronectin (Invitrogen). Cultured cells were fixed in 4% paraformaldehyde for 10 minutes, rinsed 3x in phosphate buffered saline, and permeabilized with 0.1% Triton X-100 in PBS for 15 minutes. Cells were then blocked in 5% bovine serum albumin and

subsequently incubated with the primary antibodies of interest overnight at 4C. Primary antibodies used for immunofluorescence were as follows: polyclonal anti-TDP-43 (Proteintech) 1:500, mouse anti-TIAR (BD Biosciences) 1:5000, polyclonal anti-V5 (Invitrogen). Secondary labeling was performed using Alexa Fluor 488- and 594-conjugated secondary antibodies, and samples were mounted using Vectashield mounting medium (Vector Laboratories).
TUNEL staining was carried out with the Click-iT® TUNEL Alexa Fluor® 488 Imaging Assay (Thermo Fisher) following the manufacturer's protocols.

1.11 Biochemical Procedures

Biotin-Switch: After cell lysis, free thiols were blocked with methyl-methanethiosulfonate. Cell extracts were precipitated with acetone and resuspended in HEN buffer with 1% SDS. Nitrosothiols were selectively reduced by ascorbate to remove the nitric oxide moiety and subsequently biotinylated with 1 mM biotin-HPDP (Pierce). Controls were performed without ascorbate to ensure specificity of the observed biotinylated bands. The biotinylated proteins were pulled down with streptavidin–agarose beads and analyzed by immunoblotting.

Fractionation: Cells from six-well culture dishes were scraped into 300 ml RIPA buffer (50 mM Tris pH 8.0, 150 mM NaCl, 1% NP-40, 5 mM EDTA, 0.5% sodium deoxycholate, 0.1% SDS). Samples were mechanically separated using needle aspiration, then centrifuged at 14,000 RPM for 10 minutes. The resulting

insoluble pellet was washed 1x in RIPA buffer, then suspended in 100uL of urea buffer (8M urea, 1% Triton X-100 in PBS).

Greiss Reaction: 72 hours after transfection with WT TDP-43, an addition with L-NAME where indicated, 100uL of media was removed and treated with Griess reagent (ThermoFisher). 30 minutes later color change was quantified using a plate reader at 562nm.

Recombinant protein: Recombinant 1-265 TDP-43 was cloned from pcDNA-TDP-43-V5 into pET28a-His plasmid using the following primers: 5′-CGCGGGCCCGGGATCCATGTCTGAATATATTCGG-3′ and 5′-GTCGACCCGGGAATTCTTAATTGTGCTTAGGTTCGGCA-3′. Plasmids were transformed into BL-21 ecoli and protein production was induced at O.D.600 of 0.7 via 1mM IPGAL overnight at RT. Bacteria were harvested by centrifugation 15 min 3,000xg at 4C and the cell pellet was lysed with 20mM HEPES (pH 7.5), 1M NaCl, 10% glycerol, 30mM imidazole and 5mM 2-mercaptoethanol. After sonication and centrifugation for 20min at 20,000xg, the supernatant was incubated with HisPur Colbalt Resin (Thermo Fisher) for 1hr at RT. Beads were then washed 3x with tris buffer and protein was eluted using 50mM imidazole in tris buffer. Protein was purified using Zeba desalting columns into TBS buffer.

Top Down Mass Spectometry: Measurements were performed on an LTQ-Orbitrap mass spectrometer (Thermo Electron) in the positive ion mode.

Recombinant 1-265 TDP was treated with 100uM SNOC for 20 minutes where indicated and the sample was dissolved in methanol/water with 0.5% formic acid immediately before analysis. Sample concentration was 100 fmol/µl. A sample volume of 0.5 µl was delivered to the mass spectrometer using a NanoMate 100 system (Advion Biosciences, Ithaca, NY). Mass was determined by direct calculation from the peak positions and charge states.

DAF-FM: Cortical neurons were incubated with 10ng recombinant TDP-43 overnight then washed 3x in PBS. Cultures were incubated with ACSF containing 2.5-5 µM DAF-FM diacetate for 15 minutes at room temperature in dark then washed 2x with ACSF. Slices were then imaged with epifluorescence deconvolution microscopy. Image analysis was performed using SlideBook software (Intelligent Imaging Innovations) to acquire fluorescence intensity.

Quantitative RT-PCR: RNA was prepared from cell lysate using MirVana (Invitrogen) cDNA synthesis kits (Superscript III, Invitrogen) according to the manufacturer's protocol. RT-PCR was carried out using the Roche LC480 PCR System with Sybr Green. Q-PCR conditions used were 95°C for 10 min, followed by 40 cycles of denaturing at 95°C for 15s, and annealing/extension at 60°C for 1 min, in 20µl reaction volume. All primers for QRT–PCR were from Applied Biosystems (Taqman Gene Expression Assay System). Primers used were as follows: HDAC6 forward: CGCACAGGGCTGGTCTATG, HDAC6 reverse: TGGTGGCTGTCCCACAAGTT. 18S was used as reference gene.

Chapter 2: TDP-43 Propagation

2.1 Rationale

Clinically, ALS presents with a focal point of onset which proceeds to spread along the neuroanatomical tract (Ravits & La Spada, 2009). The spread of symptomology is mirrored by pathological spread of motor neuron degeneration and cell death until the patient succumbs. This spread is increasingly recognized as a characteristic of neurodegenerative disease. Accumulating evidence has implicated prion-like pathogenesis in a variety of neurodegenerative diseases, including ALS (Brundin, Melki, & Kopito, 2010).

Prion disease is a protein misfolding disorder characterized by self-templating aggregation and propagation of PrP (Aguzzi, Heikenwalder, & Polymenidou, 2007). These misfolded PrP polymers form distinctive structures of amyloid cross beta sheets, which are able to seed further accumulations by inducing monomers to adopt the same conformation. They are transmissible from cell to cell, moving throughout the CNS and leading to neuronal degeneration and eventually death (Kanouchi, Ohkubo, & Yokota, 2012). While the mechanism of toxicity is unclear, the ability of misfolded protein to induce further aggregation is increasingly emerging as an underlying theme in a wide variety of neurodegenerative disease – associated proteins, such as Abeta and tau in Alzheimer's Disease, alpha-synucleain in Parkinson's Disease, the polyglutamine diseases, such as Huntington's Disease, and, increasingly, TDP-43 in ALS

(Fuentealba et al., 2010; J. L. Guo et al., 2013; Heilbronner et al., 2013; Robinson et al., 2013).

Pathological cytoplasmic inclusions of the protein TDP-43, an RNA-binding protein (RBP), are the pathological hallmark seen in virtually all sporadic ALS, and mutations in the TARDBP gene that encodes TDP-43 are directly linked to ALS. The protein itself exhibits substantial prion-like qualities: Aggregation of TDP-43 in ALS / FTD raises intriguing possibilities in disease pathogenesis, considering TDP-43 itself exhibits substantial prion-like qualities: The C-terminal domain of TDP-43 has a proposed prion-like structure due to its asparagine and glutamine rich sequence (Fuentealba et al., 2010) and, intriguingly, essentially all ALS-causing genetic mutations in TARDBP are clustered in this 3´ region (Pesiridis et al., 2009). Recombinant TDP-43 has been shown to induce aggregation in cell culture via an apparent seeding mechanism (Furukawa et al., 2011), as has insoluble TDP-43 from FTD and ALS patient CNS ((Nonaka et al., 2013). These reactions also resulted in toxicity and cell death in the target cells. Although several models of TDP-43 mediated toxicity have been proposed (Janssens & Van Broeckhoven, 2013; Nonaka et al., 2009) (Brettschneider et al., 2014), the mechanisms of TDP-43 propagation and aggregation are still unclear and very little attention has been directed to elucidating the biology of its propagation. In particular, the mechanisms of TDP-43 release and uptake remain unclear. It is important to develop models for TDP-43 aggregation and prion-like propagation through the nervous system to better

understand the mechanisms of ALS pathogenesis and tailor future therapeutic approaches.

There is a specific need to assays that replicate the propagation of TDP-43 in a high-throughput manner. To date, attempts to demonstrate TDP-43 propagation using cell culture models have either relied on protein transfection reagents (Nonaka et al., 2013) or have been low – yield enough to be impractical for use in a high-throughput manner (Feiler et al., 2015).

To this end, we have initiated the development of a high throughput TDP-43 propagation technique that can be quantified using both immunofluorescence and FACs.

Results

2.2 Stable Expression of TDP-43mCH in HEK FRT.

Transient transfection of TDP-43-mCH into HEK cells indicated that non-transfected cells were capable of TDP-43 uptake, as mCH fluorescent granules were observed in non-transfected cells (Fig 7A). In order to investigate this model, we stably expressed TDP-43-mCH in HEK FRT cell lines. Stable, doxycycline inducible overexpression of TDP-43-mCH resulted in a measureable increase in insoluble TDP-43 after dox induction (Fig 7C).

2.3 Experimental Plan

We utilized both the TDP-43-mCH HEK FRT cell line and a previously described HEK line where a GFP tag was inserted in the C-terminal end of

G3BP. G3BP is a stress granule marker which is diffusely cytoplasmic, but localizes to stress granules during periods of cell stress (Wheeler, Matheny, Jain, Abrisch, & Parker, 2016). We co-plated both cell lines and examined G3BP-GFP positive cells by both FACS and microscopy for co-localization of mCh and GFP signal (Fig 7B).

2.4 TDP-43-mCH Localization in G3BP-GFP cells by Microscopy

TDP-43-mCH signal was detected in HEK cells expressing G3BP-GFP (Fig 8A) using fluorescent microscopy. Intriguingly, when the cells were treated with 500mM sodium arsenite for one hour, TDP-43-mCH was observed to co-localize with G3BP-GFP positive stress granules.

2.5 TDP-43-mCH Localization in G3BP-GFP cells by FACS

Both cell lines were co-cultured for 3 days, then submitted for FACS analysis. After gating, FACS showed that 0.8% of cells were by both red and green channels. Cells that were stressed using 500mM sodium arsenite showed a mild increase to 1.2% of cells. However, when cells were stressed and allowed to recover for 72 hours before FACS sorting a significant increase in the number of cells showing both fluorescent signals was detected (Figure 8B). In cells exposed to 500mM sodium arsenite for 1 hour, 15% of cells had both mCH and GFP signals. Those exposed to a milder stress, 200mM of sodium arsenite for 20minuts, 8% of cells were detected by both channels.

2.6 Discussion

The propagation of misfolded TDP-43 has been strongly implicated in the pathogenesis of ALS and FTD, however the mechanisms behind this propagation are poorly understood (Kanouchi et al., 2012). Here we present both evidence that TDP-43 is capable of significant intercellular transmission and also a model that can be used to detect factors that contribute to TDP-43 propagation. By stably expressing doxycycline-inducible TDP-43-mCh in HEK cells we can avoid the use of transfection reagents, which may complicate any analysis of downstream propagation mechanism. Also this model allows us to maximize our signal detected by FACS, as all cells will either express mCH, GFP, or both signals.

Further, our evidence indicates that G3BP positive stress granules, indirectly implicated in the early stages of ALS pathogenesis (Dewey et al., 2012; Shukla & Parker, 2016), may be linked to TDP-43 propagation. Stress granules are dynamic complexes of untranslated mRNA and protein that form when the cell is experiencing a period of cytotoxic stress (Wheeler et al., 2016). RNA misregulation is a major theme in ALS / FTD: 1. The primary / only pathological hallmark of ALS is TDP-43 aggregation, with mutations in TDP-43 being causative (Sreedharan et al., 2008) (Daoud et al., 2009). 2. RNA binding proteins generally are associated in ALS pathogenesis, as many ALS-causing mutations occur in RBPs, leading to RNA misregulation (Nussbacher et al., 2015) (Mohagheghi et al., 2016). 3. The most common genetic cause of ALS / FTD is the C9orf72 hexanucleotide repeat expansion, which triggers the production of

RNA foci in the nucleus in the cells of patients with the disease (DeJesus-Hernandez et al., 2011). Previous studies have suggested stress granules as a site of the initiation of protein aggregation in ALS / FTD, as RNA binding proteins which contain disease-causing mutations have also been shown to co-localize to stress granules and may contribute to their stability (Aulas & Vande Velde, 2015; K. H. Lee et al., 2016; Molliex et al., 2015). Our results indicate that non-native TDP-43 may be able to co-localize with stress granules in target cells, which may contribute to stress granule stability and the pathogenesis of ALS / FTD.

Sodium arsenite is a well-known oxidative / nitrosative stressor which acts via multiple pathways within the cell and is known to promote both stress granule formation and TDP-43 insolubility (Colombrita et al., 2009; McDonald et al., 2011). Many markers indicative of oxidative stress are present in affected tissue of patients with ALS / FTD (Islam, 2017; Liu-Yesucevitz et al., 2010). Our data suggests that it may be a contributing factor in the pathogenic propagation of TDP-43, as propagation in our model was positively associated with increasing sodium arsenite stress.

Overall, we have presented evidence that TDP-43 is capable of propagating in a quantifiable manner and that we can use our model to identify factors contributing to TDP-43 spread. Future uses of this model include quantifying the contributions of TDP-43 mutations to propagation and screening other cytotoxic factors that may promote pathogenic propagation. Further, this data suggests that screening for factors that reduce TDP-43 the transmissibility of TDP-43 to spread to new treatments for patients with ALS / FTD.

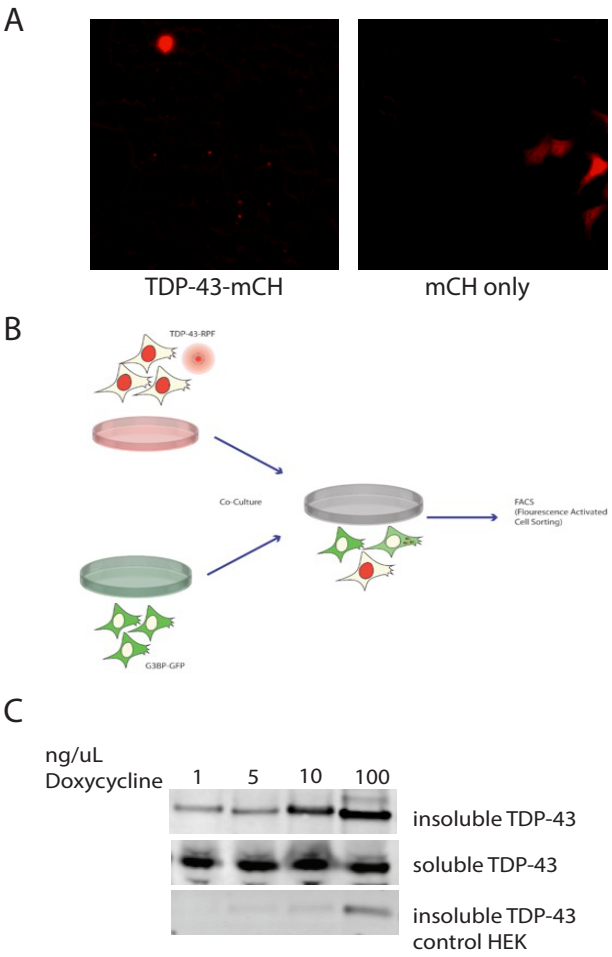

Figure 7: Rationale and Design of Experimental Plan 1A: Cells transiently transfected with TDP-mCH show inclusions in non-transfected cells. 1B Experimental plan: cells stably expressing TDP-43-mCH are co-plated with HEK cells stably expressing G3BP-GFP. These co-plated cells can be assessed by microscopy and FACS analysis. 1C: HEK line stably expressing TDP-43mCH is exposed to increasing amounts of doxycycline, cell lysate is fractionated and probed for TDP-43 (Proteintech) by Western Blot.

A

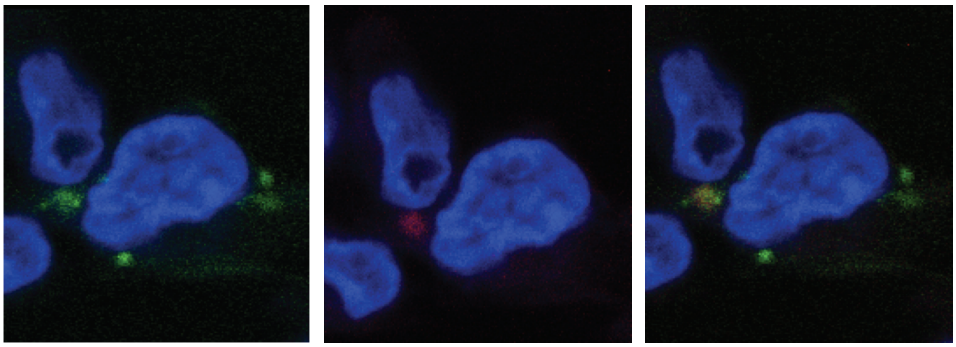

GFP signal mch signal merge signal

B

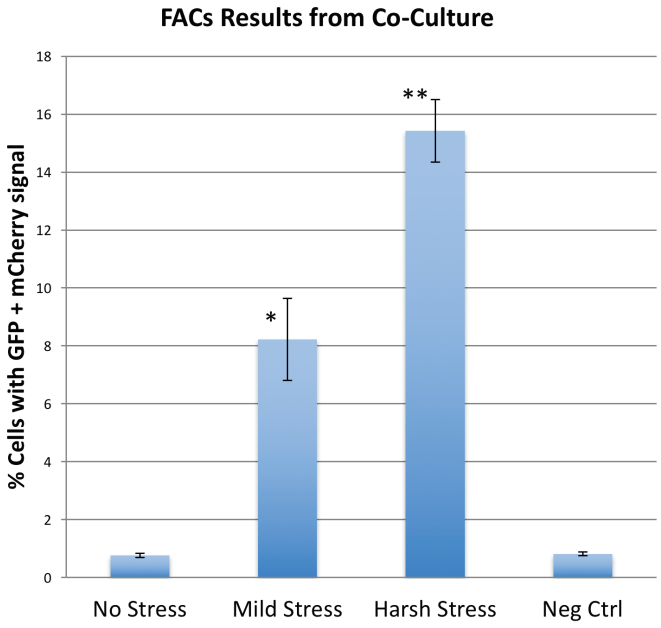

Figure 8: Quantification of TDP-43-mCH inclusions in non-native HEK 2A: Cells expressing G3BP-GFP show TDP-43-mCH positive inclusions HEK G3BP-GFP cells co-cultured with TDP-43-mCH are stressed with sodium arsenite and demonstrate TDP-43-mCH co-localization with G3BP-GFP stress granules. 2B: FACS data gating by PE-YG-A (red) and FITC-A (green). Cells were stressed and immediately processed for FACS. 2C FACS data gating by PE-YG-A (red) and FITC-A (green). Cells were stressed, allowed to recover for 72 hours and processed for FACS.

Materials / Methods

2.7 Creation of HEK293-FRT Stable Cell Line : TDP-43-mCH was generated from pcDNA3.1 TDP-43-V5, previously described. TDP-43-mCH was then subcloned into the FRT backbone. FLP-In-293 cells were used (Thermo Fisher). Cells were grown in DMEM supplemented with 10% FBS, and 1% L-glutamine and passaged using TrypLE select (Thermo Fisher). For stable cell line generation, 1x106 cells were plated into each well of a 6 well plate, then transfected with Lipofectamine 3000 (Invitrogen) and 3µg of pOG44 + 1µg of plasmid containing FRT TDP-43-mCH. 48 hours after transfection cells were split into 10cm dishes and supplemented with 100µg/ml puromycin until colonies appeared, which were then passaged and expanded.

2.8 Co-Culture: TDP-43-mCH expressing cells and G3BP-GFP cells were passaged and plated 5x104 cells onto each well of a 24 well plate. They were grown in DMEM supplemented with 10% FBS, and 1% L-glutamine.

2.9 Sodium Arsenite Treatment: 24 hours after cells were co-plated, they were stressed with either 200mM or 500mM sodium arsenite for the times indicated. After the time indicated, the media was aspirated, the cells were washed 2x with PBS and fresh media was added. The cells were then allowed to recover for the times indicated.

2.10 Fractionation: Cells from six-well culture dishes were scraped into 300 ml RIPA buffer (50 mM Tris pH 8.0, 150 mM NaCl, 1% NP-40, 5 mM EDTA, 0.5% sodium deoxycholate, 0.1% SDS). Samples were mechanically separated using needle aspiration, then centrifuged at 14,000 RPM for 10 minutes. The resulting insoluble pellet was washed 1x in RIPA buffer, then suspended in 100uL of urea buffer (8M urea, 1% Triton X-100 in PBS).

FACS: cells were lifted from the plates using TryplE and resuspended 1mL PBS. They were then passed through a 40uM cell strainer (Corning) to ensure single cells. The were then sorted in FITC (green) and (red) channels using

Chapter 3: Localization and Degradation of RNA foci using CRISPR / Cas9

3.1 Rationale

Microsatellite repeat-expansion diseases are disorders produced by an expansion of short repetitive nucleotide base sequences within the genome, and are nearly entirely neurological or neuromuscular in nature (Belzil et al., 2013).

Myotonic Dystrophy is a disease affecting multiple organ systems in which pathology develops in skeletal and cardiac muscle in addition to the CNS (Cho & Tapscott, 2007). Symptoms include myotonia, progressive weakness, cardiac arrhythmias, ocular cataracts, insulin insensitivity, hypogammaglobulinemia, hypersomnia, and cerebral atrophy. In an unaffected person, the DMPK gene contains between 5-34 copies of the CTG repeat. In a DM1 patient, however, the gene may have over 1000 CTG repeats (Krzyzosiak et al., 2012). DM2 patients, a slightly less common DM variant, have expanded CCTG repeats in the ZNF9 gene (P. Guo & Lam, 2016). This expanded nuclear transcript is maintained as RNA foci within the nucleus. These foci sequester a variety of proteins capable of binding RNA, including HNRP, STAU1, CUGBP1 and ETR3-like (CELF), and muscleblind- like (MBNL) (Goodwin et al., 2015). Sequestration of the MBNL-family of proteins appears to be particularly disruptive, as MBNL KO mice recapitulate many important aspects of DM1, while overexpression of MBNL1 leads to a reversal of symptoms in CUG repeat-expressing mice (K. Y. Lee et al., 2013). The sequestration of MBNL and other RNA binding proteins leads to

misregulation of alternative splicing, which contributes to the multi-systemic nature of this disease (Vuong, Black, & Zheng, 2016).

The C9orf72 hexanucleotide repeat expansion occurs in the first intron in the C9orf72 gene and is the most common genetic causes of both familial and sporadic ALS (Mackenzie et al., 2014). Unaffected people may carry up to 30 copies of this repeat, while those with the repeat expansion may carry over 1000 (DeJesus-Hernandez et al., 2011). However in those affected, the number of repeats does not correlate with disease onset or severity (Haeusler et al., 2016). There are three main hypotheses regarding the mechanism of cell stress / death in the C9 repeat expansion: 1. Loss of function of the C9orf72 protein. The function of C9orf72 is not clear, but the protein has some homology with proteins involved in shuttling (Mackenzie et al., 2014). There are multiple isoforms, as the protein can be alternatively spliced (Almeida et al., 2013). However, C9orf72 knockout mice do not recapitulate the effects of disease (Koppers et al., 2015). This makes loss of C9orf72 function an unlikely primary cause of the symptoms of ALS / FTD. 2. Toxic RNA foci: The accumulated RNA foci may have a toxic gain of function which induces cell stress, or may be sequestering required RNA binding proteins in the nucleus, as in DM1 (Haeusler et al., 2016). 3. Toxic dipeptide repeats: the expansion transcript is translated in both the sense (GGGGCC) and antisense (CCCCGG) direction via repeat-associated, non-ATG dependent (RAN) translation, five dipeptide repeats – three in each direction (GP is present in both directions) (Mackenzie et al., 2013) (Cleary & Ranum, 2014).These dipeptide repeats typically localize to the cytoplasm, where they co-

localize with p62 but not TDP-43 (Mackenzie et al., 2013). The most common DPR, GP, is correlated with disease severity (Cooper-Knock et al., 2015). However, the DPRs localize to a wide variety of cell types, not just those associated with disease, confounding attempts to elucidate disease mechanism.

Both DM1 and C9 ALS/FTD are neurodegenerative diseases featuring RNA foci accumulation in the nucleus (Belzil et al., 2013). Much about the etiology of these diseases remains unclear, however the targeting of the RNA foci is an intriguing research area. We have recently reported a modified version of CRISPR / Cas9 gene editing technology that is capable of binding RNAs.

As was shown in (Nelles et al., 2016), rCas9 fused to GFP is capable of tracking endogenous mRNA into stress granules – RNA dense structures which form during periods of cell stress – in live cells. This RNA tracking method is superior to previously established RNA visualization techniques: It allows unique specification in the transcriptome, does not rely on delicate microinjection procedures, and targets endogenous, unmodified RNA. The system primary relies on correctly targeted guide RNAs, meaning it is extremely adaptable for a wide range of applications.

rCas9's programmable targeting make it an ideal candidate to bind and modify disease-associated RNA foci in live cells. The exact mechanisms by which RNA foci in C9 ALS / FTD and DM1 induce cell toxicity are not clear, but by targeting these foci we may be able to reduce the associated cytotoxicity. Further work into the uses of rCas9 in RNA targeting may yield important findings relevant to the treatment of many microsatellite repeat expansion diseases.

Results

3.2 rCas9 is capable of localizing DM associated repeat foci

We first tagged rCas9 utilized the rCasGFP construct described in (Nelles et al., 2016) (Fig. 9A). After transfection with CTG150 repeats and CCTG300 repeats, COSM6 cells were probed by FISH. As a control, we used guide RNA targeted to a sequence which does not exist in eukaryotic cells. When rCas9GFP was co-transfected with CTG and CCTG repeats, the GFP signal was diffusely cytoplasmic and did not co-localize with RNA foci. However when rCasGFP was transfected with correctly targeting guide RNA it was able to co-localize with the RNA foci (Figure 9B). PAM sequence was not required for this co-localization.
rCasPIN is able to eliminate RNA foci

In order to facilitate possible degradation of disease-causing RNA foci, we fused the PIN domain, an endonuclease which cleaves single-stranded RNA, to rCas9 (rCasPIN) (Fig 9A). As in the rCasGFP experiments, when rCasPIN transfected with nontargeting guide resulted in minimal disruption to RNA foci. When cells transfected with CTG, CCTG and GGGGCC RNA repeats were transfected with rCasPIN and correctly targeted guide, we observed efficient depletion of RNA foci by FISH (Figure 10A,B,C). To confirm our quantification, we carried out northern blots to probe for the repeat RNA signal (Fig 10 E,F,G). A strong signal was detected when non-targeting guide was used, which was almost completely depleted using a guide targeting the indicated repeat sequences.

3.3 rCasPIN can eliminate RNA foci in patient cells

In order to target endogenous RNA foci in a MRE context, we utilized primary DM1 myoblasts from patient muscle biopsy and primary DM2 fibroblasts. We constructed lentiviral vectors carrying the indicated guide RNA (U6 promoter) and rCas9PIN (EFS promoter). Patient cells were infected with lentivirus carrying either nontargeting or MRE targeting guide then selected using puromycin. While the use of nontargeting guide lentivirus did not reduce the number of cells expressing RNA foci observed by FISH, the patient cells infected with targeting rCas9 lentivirus displayed a dramatic loss of observed RNA foci (Figure 11 A, C). This was confirmed by northern blot, where MRE RNA levels reduced to levels comparable to control cells (Fig. 11B). This demonstrates that our rCas9PIN and guide targeting system is able to almost completely eliminate endogenous RNA foci in the context of MRE patient cells.

3.4 rCas9PIN Corrects Toxic Effects of RNA Foci

MBNL1 sequestration by CUG repeat RNA in the nucleus is a major contributing factor to DM1 pathogenesis, resulting in the loss of MBNL1 splicing function and widespread alternative splicing (AS) dysregulation. In order to determine if degradation of the DM1 associated repeat RNA foci would reduce MBNL1 sequestration, and subsequently reduce AS, we first transfected COSM6 cells with CTG repeats and GFP-tagged MBNL1. We then co-transfected these cells with rCasPIN and targeting or nontargeting guide RNA. In the nontargeting

condition we observed that MBNL1 co-localized with the RNA foci, however it regained its typical diffuse pattern in the targeting condition (Figure 12A). This indicated that degradation of RNA foci using rCasPIN may be able to rescue cells from toxic downstream effects of RNA foci.

We further observed in patient myoblasts infected with lentiviral rCasPIN and the indicated guides that endogenous MBNL1 was redistributed in the targeting guide conditions (Figure 12B). By conducting RT-PCR on patient myoblasts using primers flanking known alternatively spliced exons in DM1, we were able to observe a correction of the DM1 specific AS pattern to that of control cells when targeting guides were used (Figure 12C). This indicates that rCasPIN is able to correct toxic downstream events via MRE RNA degradation.

3.5 rCas9 mediated RNA degradation is mediated by direct RNA binding

In order to address whether rCas9 is directly binding repeat RNA, we mixed cell lysate containing radiolabeled CUG RNA with lysate containing rCasGFP and guide RNA, then used a GFP antibody for pull down. Only when using correctly targeting guide did we observe CUG RNA pull down with rCasGFP, indicating it is being directly bound (Figure 13A).

To determine if rCas9 was inhibiting RNA foci development via DNA binding, we assembled guide RNA targeting the non-template DNA strand in the CTG repeat expansion, a sequence present only in the encoding DNA and not in the transcribed CTG repeat RNA. We chose three DNA-targeting guide RNAs that target the highest-quality non-canonical PAMs present on the non-template

DNA strand: 5'-CTG and 5'-TGC. We compared the ability of these sgRNAs to mediate the loss of CTGexp RNA foci compared to the sgRNA targeting CUGexp RNA used elsewhere in this work. We observed no loss of RNA foci in the presence of the DNA-targeting sgRNAs (Figure 13B).

3.6 Discussion

To date, no FDA approved treatments targeting RNA foci in MRE diseases exist. Symptomatically targeted treatments are unable to address disease etiology and therefore do not impact patient mortality, highlighting the need for potential therapeutics that directly engage RNA foci in MRE disorders (Wojciechowska, Taylor, Sobczak, Napierala, & Krzyzosiak, 2014). Antisense oligonucleotides have demonstrated potential in mouse models and ASOs against the C9orf72 repeat expansion are being developed by Ionis Pharmaceuticals (Jiang et al., 2016). However, targeting ASOs to the correct tissue type has proved challenging and has contributed to Ionis' recent phase 2 failure using ASOs targeting DM1 repeat sequences. RNAi can be packed into viral delivery systems, but the RNAi does not efficiently target MRE RNA foci (Wang et al., 2015).

The mechanisms of MRE RNA toxicity are widely varied and highly dependent on their sequences, genomic context, length, and protein binding capabilities (Jazurek, Ciesiolka, Starega-Roslan, Bilinska, & Krzyzosiak, 2016; Shukla & Parker, 2016). Repeats can be in coding or noncoding regions, a variety of sizes, induce alternative splicing of nearby proteins, sequester other

proteins, be RAN translated into dipeptide repeats, and can interfere with nuclear – cytoplasmic shuttling (Cleary & Ranum, 2014; P. Guo & Lam, 2016; Krzyzosiak et al., 2012; Mackenzie et al., 2014; Sicot & Gomes-Pereira, 2013). This extensive diversity of disease mechanism within the MRE disorders can be addressed using a therapeutic which directly targets the toxic RNA.

We first set out to evaluate the use of rCas9GFP, previously characterized in Nelles 2016 tracking endogenous mRNA in living cells, to target repeat RNA sequences. Using guide RNAs with multiple frames targeting both CTG and CCTG DM associated repeat sequences, we were able to observe co-localization of rCasGFP and RNA foci by FISH, suggesting rCas9 is a technique generalizable to RNA foci (Figure 9B). Only one guide frame allowed co-localization with the CTG repeats, and two guides with the CCTG repeats, suggesting that secondary structure of the foci may limit access to guide RNAs depending on the targeting frame. Furthermore, we noted that cells transfected with high concentrations of rCasGFP resulted in the suppression of RNA foci formation. This may be due to binding of rCas9GFP resulting in destabilization of the necessary RNA and protein interactions required for foci establishment.

We next sought to determine if rCas9 could be used to cleave MRE RNA foci. To this end, we replaced the GFP from rCasGFP with a PilT N-terminus domain (PIN), an RNA endonuclease from *SMG6* which was been previously shown to cleave RNA fused to an RNA binding protein. We observed that transfection with rCasPIN and the correct guide RNAs mediated loss of MRE RNA foci in CTG, CCTG and GGGGCC conditions. Additionally, treating DM1

patient myoblasts and DM2 patient fibroblasts with lentiviral rCas9PIN and the appropriate guide RNAs resulted in near eradication of endogenous foci as seen by FISH and northern blot (Figure 10).

Muscular dystrophy is a spliceopathy – sequestration of MBNL1 leads to alternative splicing of many different mRNAs, resulting in the myriad of DM symptoms (K. Y. Lee et al., 2013). Immunofluorescence carried out in both transfected COSM6 and transduced patient myoblasts demonstrated that rCasPIN mediated cleavage of RNA foci allowed MBNL1 to regain its diffuse localization (Figure 11). RT-PCR on several exons known to be alternatively spliced in DM showed a decrease in the alternative form (Figure 11C). This demonstrates that treating patient cells with rCas9 can lead to a reduction of disease phenotype and rescue the cell from toxic downstream effects of MRE RNA foci.

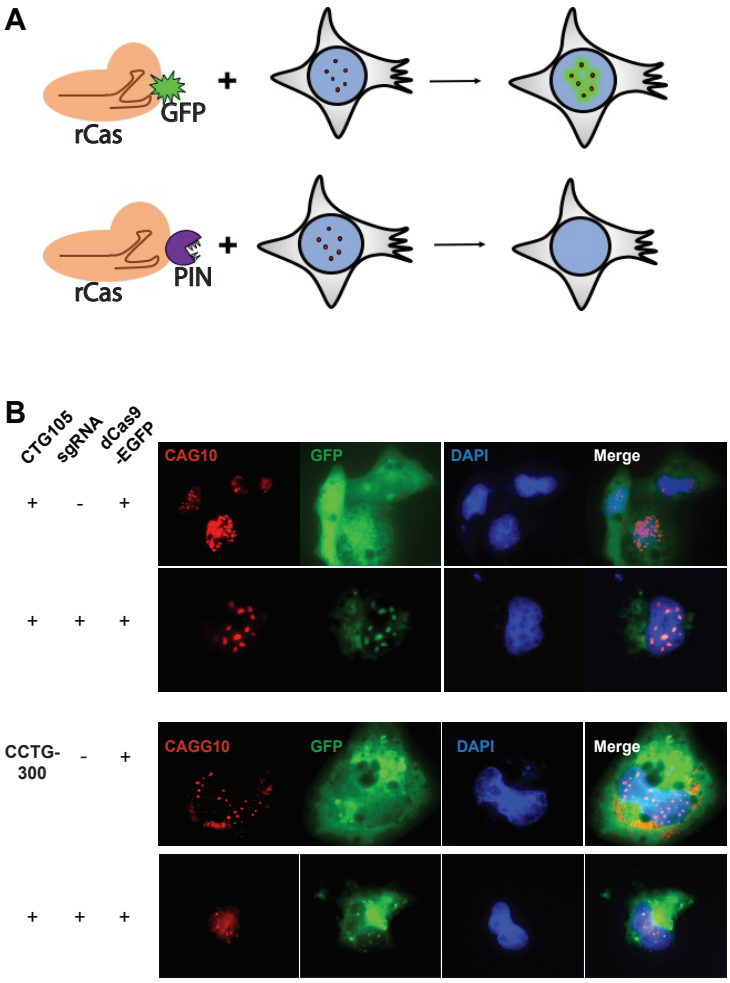

Figure 9: Targeting MRE RNA foci using rCas9

(A) Schematic demonstrating the experimental plan to track and degrade RNA foci, depending on rCas fusion state

(B) GFP fluorescence and RNA fish co-localization in COSM6 cells transfected with CTG150, along with rCasGFP and either nontargeting guide or CTG targeting guide, as indicated indicated

(C) GFP fluorescence and RNA fish co-localization in COSM6 cells transfected with CTG150, along with rCasGFP and either nontargeting guide or CCTG targeting guide, as indicated.

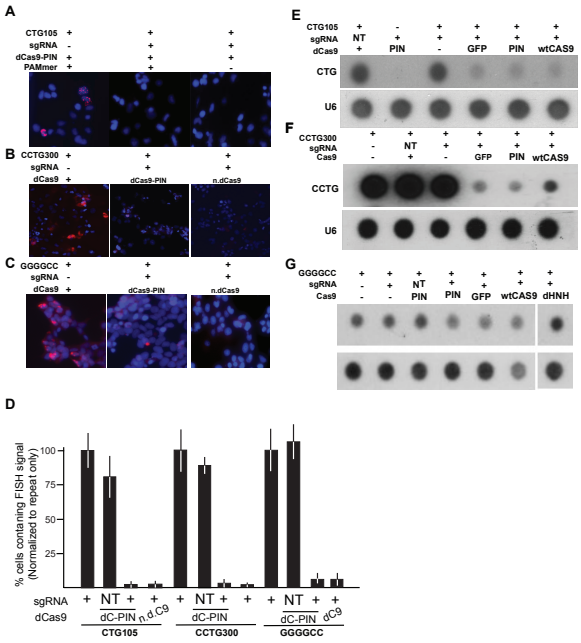

Figure 10: Degradation of RNA foci via rCasPIN

(A) RNA FISH in COSM6 cells transfected with CTG150 and either nontargeting or CTG targeting guide where indicated, with and without PAMmer

(B) RNA FISH in COSM6 cells transfected with CCTG300 and either nontargeting or CCTG targeting guide where indicated, and either rCasPIN or wild-type Cas9

(C) RNA FISH in COSM6 cells transfected with GGGGCC and either nontargeting or GGGGCC targeting guide where indicated, and either rCasPIN or wild-type Cas9

(D) Quantification of foci by FISH containing COSM6 cells after transfection with the indicated MRE, guides, and CRISPR / Cas9 plasmids

(E) Northern dot blot probing for CTG RNA in COSM6 cells transfected as indicated with MRE, guides, and CRISPR / Cas9

(F) Northern dot blot probing for CCTG RNA in COSM6 cells transfected as indicated with MRE, guides, and CRISPR / Cas9

(G) Northern dot blot probing for GGGGCC RNA in COSM6 cells transfected as indicated with MRE, guides, and CRISPR / Cas9

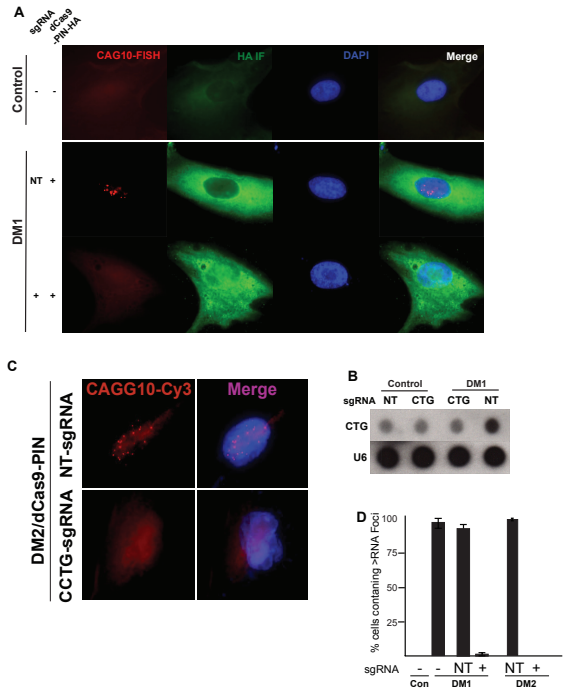

Figure 11: Degradation of RNA foci in Patient Cells

(A) RNA FISH and rCasPIN-HA immunofluorescence in DM1 myoblasts transduced with lentivirus containing rCasPIN, nontargeting or CTG targeting guide as indicated

(B) Northern dot blot quantifying CTG RNA in DM1 patient myoblasts transduced with lentivirus containing rCasPIN, nontargeting CTG targeting guide as indicated.

(C) RNA FISH signal in DM2 patient fibroblasts transduced with lentivirus containing rCasPIN and nontargeting or CTG targeting guide as indicated

(D) Quantification of RNA FISH signal in DM1 myoblasts and DM2 fibroblasts transduced with lentivirus containing rCasPIN and nontargeting or CTG targeting guide as indicated

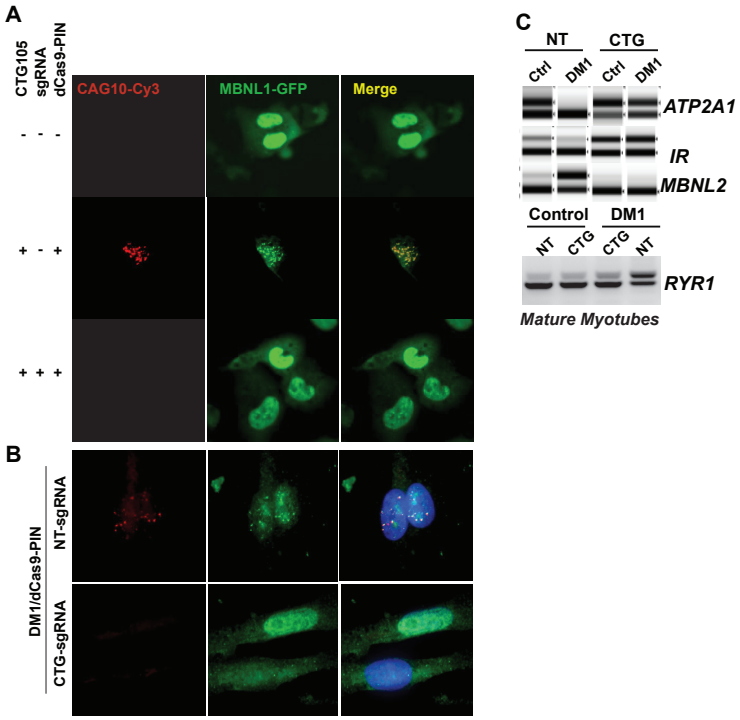

Figure 12: rCas9 Rescues From Effects of RNA Foci

(A) RNA FISH and GFP fluorescence in COSM6 cells transfected with CTG MRE and MBNL1_GFP plasmids, along with nontargeting or CTG targeting guide as indicated

(B) Colocalization of RNA FISH and immunofluorescence of MBNL1 in DM1 myoblasts transduced with lentivirus containing rCasPIN, nontargeting CTG targeting guide as indicated.

(C) RT-PCR of alternative splicing in DM1 myoblasts

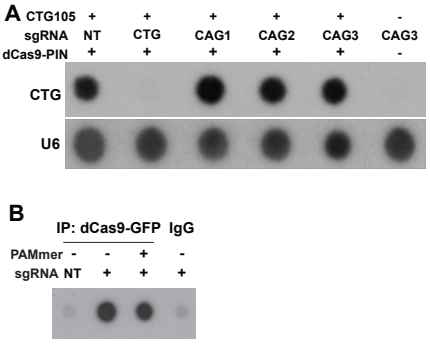

Figure 13: rCas9 RNA Degradation Mediated by RNA Binding

(A) Northern dot blot probing for CTG MRE RNA in COSM6 cells after transfection with CTG105, rCasPIN, and nontargeting, CTG, or CAG guide as indicated

(B) Immunoprecipitated anti-GFP pull down of P-32 labeled CTG105 RNA with rCasGFP and nontargeting or CTG guide as indicated

Materials and Methods

3.7 Cell Culture

COSM6 immortalized cells were cultured in DMEM with 10% fetal bovine serum. They were passaged using TrypLE (Invitrogen). Primary myoblasts were grown in complete SKGM-2 media (Lonza) and differentiated by plating at 90% confluence in DMEM + 2% horse serum (GIBCO) on a collagen coated 6- or 12-well plate. Fibroblasts were maintained in DMEM + 12% FBS. Cells were seeded in a 6-well plate prior to lentivirus infections. Myoblasts, myotubes and fibroblasts were transduced with 100X concentrated lentivirus and selected with 2ug/mL puromycin at 48 hours.

3.8 Transfections

COSM6 cells were seeded into 4-chambered glass slides at 5x10^4 cells per well for FISH. 50ng MRE, 250ng guide RNA and 250ng rCas9 plasmid was transfected in OptiMEM using Lipofectamine 3000 (Invitrogen) following the manufacturer's protocol. For GGGGCC repeats, 25ug of repeat was transfected with 250ng rCas9 (1:10 ratio). For rCasGFP imaging, 100ng of repeat was used with 50ng of rCasGFP to prevent foci degradation.

For RNA isolation 6-well plates were used, seeding cells 3x10^5 cells per well. 150ng of MRE repeat was transfected, along with 500ng of guide RNA and rCas9 plasmids. For GGGGCC, 50ng of repeat was used.

3.9 RNA Florescence in-situ hybridization (FISH)

Cells were rinsed 1x with PBS, fixed for 10min with 4%PFA, then rinsed 3x with PBS and incubated overnight at 4C in 70% ethanol. Ethanol was removed and the cells were rehydrated with wash buffer (40% formamide and 2X SSC buffer). Cells were then incubated for 20min at 37C (65C for GGGGCC repeats) in prehybridization buffer (10% dextran sulfate, 2mM ribonucleoside vanadyl complex, 2X SSC pH 5, 50% fresh & deionized RNase-free formamide, 200 ug/mL BSA, 1 mg/ml yeast tRNA, DEPC-treated water to attain final target volume) in a hybridization oven. The probes were denatured for 10minutes at 100C. The probe was then added to cold prehybridization buffer for a final concentration of 500pg/uL (1ug/uL for GGGGCC), which was immediately added to the cells. Cells were incubated with the probe for 2 hours at 37C (65C for GGGGCC) in a hyb oven. After hybridization, the cells were washed 3x for 30min each with wash buffer, then washed 1X with PBS and mounted with mounting medium containing DAPI.

3.10 Northern Blot

RNA was isolated using trizol and concentration was measured on the Nanodrop spectrophotometer. 1-5ug of total RNA was diluted in 1mM EDTA, pH 8.0 to 50ul. 30ul 20X SSC and 20ul 37% formaldehyde was added for RNA denaturation. The samples were incubated for 30 minutes at 60C, then moved to ice. Dot blots were carried out using the Biorad Bio-dot apparatus according to the manufacturer's protocol using Hybond N+ nylon membrane (GE healthcare).

The membrane was rinsed with 100ul of 20X SSC / well. The RNA samples were then pulled through the slots by the vacuum, and the membrane was again rinsed with 20X SSC. The membrane was crosslinked in the UV stratalinker (Stratagene). Expresshyb (Clonetech), pre-warmed at 50C, was used for prehybridization at 55C for 60 minutes. During prehybridization, the probe was labeled with gamma-P32 ATP (Perkin Elmer) and T4-PNK (NEB) at 37C for 30 minutes, filtered through a G-50 Illustra spin column (GE Healthcare), denatured at 100C for 10 minutes, and placed on ice. The probe was then added to the prehybridization solution at a concentration of 1ug/mL. Hybridization was done overnight and the membrane was washed with 1X with 1X SSC, 0.1 % SDS at 55C and 2X with 0.5X SSC, 0.1 % SDS at 55C. The membrane was developed with autoradiography film (Thermo Fisher) with an intensifying screen (Kodak) at -80C overnight (~16 hours).

3.11 In Vitro transcription and Immunoprecipitation

In vitro transcription of CUG repeats was carried out with MAXIscript SP6 in vitro transcription kit (Thermo) and alpha P-32 UTP (Perkin Elmer). COSM6 were transfected wither either nontargeting guide RNA and rCasGFP or CTG-targeting guide RNA and rCasGFP. 48 hours after transfection, cellular extracts were prepared in Tris-HCl pH 7.0, 0.1% Igepal and sonicated in a bioruptor. Equal amounts of RNA was mixed with cellular extract and 1mg/ml yeast tRNA for 60 minutes at 37C. Dynabeads M-280 sheep anti-rabbit (Thermo) were incubated with anti-GFP antibody (Abcam Ab290) and immunoprecipitation was

carried out for 2 hours at RT. The beads were washed with Tris-HCl, 0.1% Igepal 5X or until the IgG control sample had no detectable radiation as measured by a Geiger counter. The RNA was eluted with Proteinase K in PK buffer for 30 minutes at 37C and was blotted on Hybond N+ membrane using the Bio Dot apparatus as described above. The membrane was washed 1X with 1X SSC and developed with autoradiography film (Kodak) with an intensifying screen at -80C for 2-4 hours.

Chapter 3 is a modified adaptation of the material as it appears in: Elimination of Toxic Microsatellite Repeat Expansion RNA by RNA-Targeting Cas9. Ranjan Batra, David Nelles, Elaine Pirie, Steven Blue, Ryan Marina, Harrison Wang, Issac Alexander Chaim, James Thomas, Nigel Zhang, Vu Nguyen, Stefan Aigner, Sebastian Markmiller, Guangbin Xia, Kevin Corbett, Maurice Swanson, Gene Yeo. The dissertation author was the second author of this paper.

Bibliography

Aguzzi, A., Heikenwalder, M., & Polymenidou, M. (2007). Insights into prion strains and neurotoxicity. *Nat Rev Mol Cell Biol, 8*(7), 552-561. doi:10.1038/nrm2204

Akhtar, M. W., Sunico, C. R., Nakamura, T., & Lipton, S. A. (2012). Redox Regulation of Protein Function via Cysteine S-Nitrosylation and Its Relevance to Neurodegenerative Diseases. *Int J Cell Biol, 2012*, 463756. doi:10.1155/2012/463756

Almeida, S., Gascon, E., Tran, H., Chou, H. J., Gendron, T. F., Degroot, S., . . . Gao, F. B. (2013). Modeling key pathological features of frontotemporal dementia with C9ORF72 repeat expansion in iPSC-derived human neurons. *Acta Neuropathol, 126*(3), 385-399. doi:10.1007/s00401-013-1149-y

Andre, F. R., dos Santos, P. F., & Rando, D. G. (2016). Theoretical studies of the role of C-terminal cysteines in the process of S-nitrosylation of human Src kinases. *J Mol Model, 22*(1), 23. doi:10.1007/s00894-015-2892-x

Aulas, A., & Vande Velde, C. (2015). Alterations in stress granule dynamics driven by TDP-43 and FUS: a link to pathological inclusions in ALS? *Front Cell Neurosci, 9*, 423. doi:10.3389/fncel.2015.00423

Ayala, Y. M., Zago, P., D'Ambrogio, A., Xu, Y. F., Petrucelli, L., Buratti, E., & Baralle, F. E. (2008). Structural determinants of the cellular localization and shuttling of TDP-43. *J Cell Sci, 121*(Pt 22), 3778-3785. doi:10.1242/jcs.038950

Begg, G. E., & Speicher, D. W. (1999). Mass spectrometry detection and reduction of disulfide adducts between reducing agents and recombinant proteins with highly reactive cysteines. *J Biomol Tech, 10*(1), 17-20.

Belzil, V. V., Gendron, T. F., & Petrucelli, L. (2013). RNA-mediated toxicity in neurodegenerative disease. *Mol Cell Neurosci, 56*, 406-419. doi:10.1016/j.mcn.2012.12.006

Betarbet, R., Sherer, T. B., MacKenzie, G., Garcia-Osuna, M., Panov, A. V., & Greenamyre, J. T. (2000). Chronic systemic pesticide exposure reproduces features of Parkinson's disease. *Nat Neurosci, 3*(12), 1301-1306. doi:10.1038/81834

Brettschneider, J., Arai, K., Del Tredici, K., Toledo, J. B., Robinson, J. L., Lee, E. B., . . . Trojanowski, J. Q. (2014). TDP-43 pathology and neuronal loss in amyotrophic lateral sclerosis spinal cord. *Acta Neuropathol, 128*(3), 423-437. doi:10.1007/s00401-014-1299-6

Brundin, P., Melki, R., & Kopito, R. (2010). Prion-like transmission of protein aggregates in neurodegenerative diseases. *Nat Rev Mol Cell Biol, 11*(4), 301-307. doi:10.1038/nrm2873

Chen-Plotkin, A. S., Lee, V. M., & Trojanowski, J. Q. (2010). TAR DNA-binding protein 43 in neurodegenerative disease. *Nat Rev Neurol, 6*(4), 211-220. doi:10.1038/nrneurol.2010.18

Chiang, C. H., Grauffel, C., Wu, L. S., Kuo, P. H., Doudeva, L. G., Lim, C., . . . Yuan, H. S. (2016). Structural analysis of disease-related TDP-43 D169G mutation: linking enhanced stability and caspase cleavage efficiency to protein accumulation. *Sci Rep, 6*, 21581. doi:10.1038/srep21581

Cho, D. H., & Tapscott, S. J. (2007). Myotonic dystrophy: emerging mechanisms for DM1 and DM2. *Biochim Biophys Acta, 1772*(2), 195-204. doi:10.1016/j.bbadis.2006.05.013

Cleary, J. D., & Ranum, L. P. (2014). Repeat associated non-ATG (RAN) translation: new starts in microsatellite expansion disorders. *Curr Opin Genet Dev, 26*, 6-15. doi:10.1016/j.gde.2014.03.002

Cohen, T. J., Hwang, A. W., Unger, T., Trojanowski, J. Q., & Lee, V. M. (2012). Redox signalling directly regulates TDP-43 via cysteine oxidation and disulphide cross-linking. *Embo j, 31*(5), 1241-1252. doi:10.1038/emboj.2011.471

Colombrita, C., Zennaro, E., Fallini, C., Weber, M., Sommacal, A., Buratti, E., . . . Ratti, A. (2009). TDP-43 is recruited to stress granules in conditions of oxidative insult. *J Neurochem, 111*(4), 1051-1061. doi:10.1111/j.1471-4159.2009.06383.x

Cooper-Knock, J., Higginbottom, A., Stopford, M. J., Highley, J. R., Ince, P. G., Wharton, S. B., . . . Shaw, P. J. (2015). Antisense RNA foci in the motor neurons of C9ORF72-ALS patients are associated with TDP-43 proteinopathy. *Acta Neuropathol, 130*(1), 63-75. doi:10.1007/s00401-015-1429-9

Daoud, H., Valdmanis, P. N., Kabashi, E., Dion, P., Dupre, N., Camu, W., . . . Rouleau, G. A. (2009). Contribution of TARDBP mutations to sporadic

amyotrophic lateral sclerosis. *J Med Genet, 46*(2), 112-114. doi:10.1136/jmg.2008.062463

DeJesus-Hernandez, M., Mackenzie, I. R., Boeve, B. F., Boxer, A. L., Baker, M., Rutherford, N. J., . . . Rademakers, R. (2011). Expanded GGGGCC hexanucleotide repeat in noncoding region of C9ORF72 causes chromosome 9p-linked FTD and ALS. *Neuron, 72*(2), 245-256. doi:10.1016/j.neuron.2011.09.011

Dewey, C. M., Cenik, B., Sephton, C. F., Johnson, B. A., Herz, J., & Yu, G. (2012). TDP-43 aggregation in neurodegeneration: are stress granules the key? *Brain Res, 1462*, 16-25. doi:10.1016/j.brainres.2012.02.032

Fang, Y. S., Tsai, K. J., Chang, Y. J., Kao, P., Woods, R., Kuo, P. H., . . . Chen, Y. R. (2014). Full-length TDP-43 forms toxic amyloid oligomers that are present in frontotemporal lobar dementia-TDP patients. *Nat Commun, 5*, 4824. doi:10.1038/ncomms5824

Feiler, M. S., Strobel, B., Freischmidt, A., Helferich, A. M., Kappel, J., Brewer, B. M., . . . Weishaupt, J. H. (2015). TDP-43 is intercellularly transmitted across axon terminals. *J Cell Biol, 211*(4), 897-911. doi:10.1083/jcb.201504057

Fiesel, F. C., Voigt, A., Weber, S. S., Van den Haute, C., Waldenmaier, A., Gorner, K., . . . Kahle, P. J. (2010). Knockdown of transactive response DNA-binding protein (TDP-43) downregulates histone deacetylase 6. *Embo j, 29*(1), 209-221. doi:10.1038/emboj.2009.324

Fuentealba, R. A., Udan, M., Bell, S., Wegorzewska, I., Shao, J., Diamond, M. I., . . . Baloh, R. H. (2010). Interaction with polyglutamine aggregates reveals a Q/N-rich domain in TDP-43. *J Biol Chem, 285*(34), 26304-26314. doi:10.1074/jbc.M110.125039

Furukawa, Y., Kaneko, K., Watanabe, S., Yamanaka, K., & Nukina, N. (2011). A seeding reaction recapitulates intracellular formation of Sarkosyl-insoluble transactivation response element (TAR) DNA-binding protein-43 inclusions. *J Biol Chem, 286*(21), 18664-18672. doi:10.1074/jbc.M111.231209

Geser, F., Martinez-Lage, M., Kwong, L. K., Lee, V. M., & Trojanowski, J. Q. (2009). Amyotrophic lateral sclerosis, frontotemporal dementia and beyond: the TDP-43 diseases. *J Neurol, 256*(8), 1205-1214. doi:10.1007/s00415-009-5069-7

Geser, F., Martinez-Lage, M., Robinson, J., Uryu, K., Neumann, M., Brandmeir, N. J., . . . Trojanowski, J. Q. (2009). Clinical and pathological continuum of multisystem TDP-43 proteinopathies. *Arch Neurol, 66*(2), 180-189. doi:10.1001/archneurol.2008.558

Goodwin, M., Mohan, A., Batra, R., Lee, K. Y., Charizanis, K., Fernandez Gomez, F. J., . . . Swanson, M. S. (2015). MBNL Sequestration by Toxic RNAs and RNA Misprocessing in the Myotonic Dystrophy Brain. *Cell Rep, 12*(7), 1159-1168. doi:10.1016/j.celrep.2015.07.029

Gu, Z., Nakamura, T., & Lipton, S. A. (2010). Redox reactions induced by nitrosative stress mediate protein misfolding and mitochondrial dysfunction in neurodegenerative diseases. *Mol Neurobiol, 41*(2-3), 55-72. doi:10.1007/s12035-010-8113-9

Guo, J. L., Covell, D. J., Daniels, J. P., Iba, M., Stieber, A., Zhang, B., . . . Lee, V. M. (2013). Distinct alpha-synuclein strains differentially promote tau inclusions in neurons. *Cell, 154*(1), 103-117. doi:10.1016/j.cell.2013.05.057

Guo, P., & Lam, S. L. (2016). Unusual structures of CCTG repeats and their participation in repeat expansion. *Biomol Concepts, 7*(5-6), 331-340. doi:10.1515/bmc-2016-0024

Haeusler, A. R., Donnelly, C. J., & Rothstein, J. D. (2016). The expanding biology of the C9orf72 nucleotide repeat expansion in neurodegenerative disease. *Nat Rev Neurosci, 17*(6), 383-395. doi:10.1038/nrn.2016.38

Heilbronner, G., Eisele, Y. S., Langer, F., Kaeser, S. A., Novotny, R., Nagarathinam, A., . . . Jucker, M. (2013). Seeded strain-like transmission of beta-amyloid morphotypes in APP transgenic mice. *EMBO Rep, 14*(11), 1017-1022. doi:10.1038/embor.2013.137

Hess, D. T., Matsumoto, A., Kim, S. O., Marshall, H. E., & Stamler, J. S. (2005). Protein S-nitrosylation: purview and parameters. *Nat Rev Mol Cell Biol, 6*(2), 150-166. doi:10.1038/nrm1569

Islam, M. T. (2017). Oxidative stress and mitochondrial dysfunction-linked neurodegenerative disorders. *Neurol Res, 39*(1), 73-82. doi:10.1080/01616412.2016.1251711

Janssens, J., & Van Broeckhoven, C. (2013). Pathological mechanisms underlying TDP-43 driven neurodegeneration in FTLD-ALS spectrum disorders. *Hum Mol Genet, 22*(R1), R77-87. doi:10.1093/hmg/ddt349

Jazurek, M., Ciesiolka, A., Starega-Roslan, J., Bilinska, K., & Krzyzosiak, W. J. (2016). Identifying proteins that bind to specific RNAs - focus on simple repeat expansion diseases. *Nucleic Acids Res, 44*(19), 9050-9070. doi:10.1093/nar/gkw803

Jiang, J., Zhu, Q., Gendron, T. F., Saberi, S., McAlonis-Downes, M., Seelman, A., . . . Lagier-Tourenne, C. (2016). Gain of Toxicity from ALS/FTD-Linked Repeat Expansions in C9ORF72 Is Alleviated by Antisense Oligonucleotides Targeting GGGGCC-Containing RNAs. *Neuron, 90*(3), 535-550. doi:10.1016/j.neuron.2016.04.006

Kamel, F., Umbach, D. M., Bedlack, R. S., Richards, M., Watson, M., Alavanja, M. C., . . . Sandler, D. P. (2012). Pesticide exposure and amyotrophic lateral sclerosis. *Neurotoxicology, 33*(3), 457-462. doi:10.1016/j.neuro.2012.04.001

Kanouchi, T., Ohkubo, T., & Yokota, T. (2012). Can regional spreading of amyotrophic lateral sclerosis motor symptoms be explained by prion-like propagation? *J Neurol Neurosurg Psychiatry, 83*(7), 739-745. doi:10.1136/jnnp-2011-301826

Koppers, M., Blokhuis, A. M., Westeneng, H. J., Terpstra, M. L., Zundel, C. A., Vieira de Sa, R., . . . Pasterkamp, R. J. (2015). C9orf72 ablation in mice does not cause motor neuron degeneration or motor deficits. *Ann Neurol, 78*(3), 426-438. doi:10.1002/ana.24453

Krzyzosiak, W. J., Sobczak, K., Wojciechowska, M., Fiszer, A., Mykowska, A., & Kozlowski, P. (2012). Triplet repeat RNA structure and its role as pathogenic agent and therapeutic target. *Nucleic Acids Res, 40*(1), 11-26. doi:10.1093/nar/gkr729

Lee, E. B., Lee, V. M., & Trojanowski, J. Q. (2011). Gains or losses: molecular mechanisms of TDP43-mediated neurodegeneration. *Nat Rev Neurosci, 13*(1), 38-50. doi:10.1038/nrn3121

Lee, K. H., Zhang, P., Kim, H. J., Mitrea, D. M., Sarkar, M., Freibaum, B. D., . . . Taylor, J. P. (2016). C9orf72 Dipeptide Repeats Impair the Assembly, Dynamics, and Function of Membrane-Less Organelles. *Cell, 167*(3), 774-788.e717. doi:10.1016/j.cell.2016.10.002

Lee, K. Y., Li, M., Manchanda, M., Batra, R., Charizanis, K., Mohan, A., . . . Swanson, M. S. (2013). Compound loss of muscleblind-like function in myotonic dystrophy. *EMBO Mol Med, 5*(12), 1887-1900. doi:10.1002/emmm.201303275

Liu-Yesucevitz, L., Bilgutay, A., Zhang, Y. J., Vanderweyde, T., Citro, A., Mehta, T., . . . Wolozin, B. (2010). Tar DNA binding protein-43 (TDP-43) associates with stress granules: analysis of cultured cells and pathological brain tissue. *PLoS One, 5*(10), e13250. doi:10.1371/journal.pone.0013250

Lopez-Sanchez, L. M., Lopez-Pedrera, C., & Rodriguez-Ariza, A. (2014). Proteomic approaches to evaluate protein S-nitrosylation in disease. *Mass Spectrom Rev, 33*(1), 7-20. doi:10.1002/mas.21373

Lukavsky, P. J., Daujotyte, D., Tollervey, J. R., Ule, J., Stuani, C., Buratti, E., . . . Allain, F. H. (2013). Molecular basis of UG-rich RNA recognition by the human splicing factor TDP-43. *Nat Struct Mol Biol, 20*(12), 1443-1449. doi:10.1038/nsmb.2698

Mackenzie, I. R., Arzberger, T., Kremmer, E., Troost, D., Lorenzl, S., Mori, K., . . . Neumann, M. (2013). Dipeptide repeat protein pathology in C9ORF72 mutation cases: clinico-pathological correlations. *Acta Neuropathol, 126*(6), 859-879. doi:10.1007/s00401-013-1181-y

Mackenzie, I. R., Frick, P., & Neumann, M. (2014). The neuropathology associated with repeat expansions in the C9ORF72 gene. *Acta Neuropathol, 127*(3), 347-357. doi:10.1007/s00401-013-1232-4

McDonald, K. K., Aulas, A., Destroismaisons, L., Pickles, S., Beleac, E., Camu, W., . . . Vande Velde, C. (2011). TAR DNA-binding protein 43 (TDP-43) regulates stress granule dynamics via differential regulation of G3BP and TIA-1. *Hum Mol Genet, 20*(7), 1400-1410. doi:10.1093/hmg/ddr021

McKhann, G. M., Albert, M. S., Grossman, M., Miller, B., Dickson, D., & Trojanowski, J. Q. (2001). Clinical and pathological diagnosis of frontotemporal dementia: report of the Work Group on Frontotemporal Dementia and Pick's Disease. *Arch Neurol, 58*(11), 1803-1809.

Mohagheghi, F., Prudencio, M., Stuani, C., Cook, C., Jansen-West, K., Dickson, D. W., . . . Buratti, E. (2016). TDP-43 functions within a network of hnRNP proteins to inhibit the production of a truncated human SORT1 receptor. *Hum Mol Genet, 25*(3), 534-545. doi:10.1093/hmg/ddv491

Molliex, A., Temirov, J., Lee, J., Coughlin, M., Kanagaraj, A. P., Kim, H. J., . . . Taylor, J. P. (2015). Phase separation by low complexity domains promotes stress granule assembly and drives pathological fibrillization. *Cell, 163*(1), 123-133. doi:10.1016/j.cell.2015.09.015

Nakamura, T., & Lipton, S. A. (2013). Emerging role of protein-protein transnitrosylation in cell signaling pathways. *Antioxid Redox Signal, 18*(3), 239-249. doi:10.1089/ars.2012.4703

Nakato, R., Ohkubo, Y., Konishi, A., Shibata, M., Kaneko, Y., Iwawaki, T., . . . Uehara, T. (2015). Regulation of the unfolded protein response via S-nitrosylation of sensors of endoplasmic reticulum stress. *Sci Rep, 5*, 14812. doi:10.1038/srep14812

Nelles, D. A., Fang, M. Y., O'Connell, M. R., Xu, J. L., Markmiller, S. J., Doudna, J. A., & Yeo, G. W. (2016). Programmable RNA Tracking in Live Cells with CRISPR/Cas9. *Cell, 165*(2), 488-496. doi:10.1016/j.cell.2016.02.054

Neumann, M., Sampathu, D. M., Kwong, L. K., Truax, A. C., Micsenyi, M. C., Chou, T. T., . . . Lee, V. M. (2006). Ubiquitinated TDP-43 in frontotemporal lobar degeneration and amyotrophic lateral sclerosis. *Science, 314*(5796), 130-133. doi:10.1126/science.1134108

Nonaka, T., Kametani, F., Arai, T., Akiyama, H., & Hasegawa, M. (2009). Truncation and pathogenic mutations facilitate the formation of intracellular aggregates of TDP-43. *Hum Mol Genet, 18*(18), 3353-3364. doi:10.1093/hmg/ddp275

Nonaka, T., Masuda-Suzukake, M., Arai, T., Hasegawa, Y., Akatsu, H., Obi, T., . . . Hasegawa, M. (2013). Prion-like properties of pathological TDP-43 aggregates from diseased brains. *Cell Rep, 4*(1), 124-134. doi:10.1016/j.celrep.2013.06.007

Nussbacher, J. K., Batra, R., Lagier-Tourenne, C., & Yeo, G. W. (2015). RNA-binding proteins in neurodegeneration: Seq and you shall receive. *Trends Neurosci, 38*(4), 226-236. doi:10.1016/j.tins.2015.02.003

Pesiridis, G. S., Lee, V. M., & Trojanowski, J. Q. (2009). Mutations in TDP-43 link glycine-rich domain functions to amyotrophic lateral sclerosis. *Hum Mol Genet, 18*(R2), R156-162. doi:10.1093/hmg/ddp303

Ravits, J. M., & La Spada, A. R. (2009). ALS motor phenotype heterogeneity, focality, and spread: deconstructing motor neuron degeneration. *Neurology, 73*(10), 805-811. doi:10.1212/WNL.0b013e3181b6bbbd

Robinson, J. L., Geser, F., Stieber, A., Umoh, M., Kwong, L. K., Van Deerlin, V. M., . . . Trojanowski, J. Q. (2013). TDP-43 skeins show properties of amyloid in a subset of ALS cases. *Acta Neuropathol, 125*(1), 121-131. doi:10.1007/s00401-012-1055-8

Sattler, R., Xiong, Z., Lu, W. Y., Hafner, M., MacDonald, J. F., & Tymianski, M. (1999). Specific coupling of NMDA receptor activation to nitric oxide neurotoxicity by PSD-95 protein. *Science, 284*(5421), 1845-1848.

Shodai, A., Morimura, T., Ido, A., Uchida, T., Ayaki, T., Takahashi, R., . . . Urushitani, M. (2013). Aberrant assembly of RNA recognition motif 1 links to pathogenic conversion of TAR DNA-binding protein of 43 kDa (TDP-43). *J Biol Chem, 288*(21), 14886-14905. doi:10.1074/jbc.M113.451849

Shukla, S., & Parker, R. (2016). Hypo- and Hyper-Assembly Diseases of RNA-Protein Complexes. *Trends Mol Med, 22*(7), 615-628. doi:10.1016/j.molmed.2016.05.005

Sicot, G., & Gomes-Pereira, M. (2013). RNA toxicity in human disease and animal models: from the uncovering of a new mechanism to the development of promising therapies. *Biochim Biophys Acta, 1832*(9), 1390-1409. doi:10.1016/j.bbadis.2013.03.002

Sreedharan, J., Blair, I. P., Tripathi, V. B., Hu, X., Vance, C., Rogelj, B., . . . Shaw, C. E. (2008). TDP-43 mutations in familial and sporadic amyotrophic lateral sclerosis. *Science, 319*(5870), 1668-1672. doi:10.1126/science.1154584

Talbot, K., & Ansorge, O. (2006). Recent advances in the genetics of amyotrophic lateral sclerosis and frontotemporal dementia: common pathways in neurodegenerative disease. *Hum Mol Genet, 15 Spec No 2*, R182-187. doi:10.1093/hmg/ddl202

Tollervey, J. R., Curk, T., Rogelj, B., Briese, M., Cereda, M., Kayikci, M., . . . Ule, J. (2011). Characterizing the RNA targets and position-dependent splicing regulation by TDP-43. *Nat Neurosci, 14*(4), 452-458. doi:10.1038/nn.2778

Usdin, K. (2008). The biological effects of simple tandem repeats: lessons from the repeat expansion diseases. *Genome Res, 18*(7), 1011-1019. doi:10.1101/gr.070409.107

Vuong, C. K., Black, D. L., & Zheng, S. (2016). The neurogenetics of alternative splicing. *Nat Rev Neurosci, 17*(5), 265-281. doi:10.1038/nrn.2016.27

Wang, J., Liang, H., Zhao, Y., Liu, X., Yang, K., & Sui, A. (2015). Construction and identification of an RNA interference lentiviral vector targeting the mouse TNF-alpha gene. *Exp Ther Med, 10*(6), 2283-2288. doi:10.3892/etm.2015.2813

Wheeler, J. R., Matheny, T., Jain, S., Abrisch, R., & Parker, R. (2016). Distinct stages in stress granule assembly and disassembly. *Elife, 5*. doi:10.7554/eLife.18413

Winton, M. J., Igaz, L. M., Wong, M. M., Kwong, L. K., Trojanowski, J. Q., & Lee, V. M. (2008). Disturbance of nuclear and cytoplasmic TAR DNA-binding protein (TDP-43) induces disease-like redistribution, sequestration, and aggregate formation. *J Biol Chem, 283*(19), 13302-13309. doi:10.1074/jbc.M800342200

Wojciechowska, M., Taylor, K., Sobczak, K., Napierala, M., & Krzyzosiak, W. J. (2014). Small molecule kinase inhibitors alleviate different molecular features of myotonic dystrophy type 1. *RNA Biol, 11*(6), 742-754.

Xie, H. R., Hu, L. S., & Li, G. Y. (2010). SH-SY5Y human neuroblastoma cell line: in vitro cell model of dopaminergic neurons in Parkinson's disease. *Chin Med J (Engl), 123*(8), 1086-1092.

Yamashita, M., Nonaka, T., Arai, T., Kametani, F., Buchman, V. L., Ninkina, N., . . . Hasegawa, M. (2009). Methylene blue and dimebon inhibit aggregation of TDP-43 in cellular models. *FEBS Lett, 583*(14), 2419-2424. doi:10.1016/j.febslet.2009.06.042